



Published in final edited form as:

Circulation. 2026 April 07; 153(14): 1060–1076. doi:10.1161/CIRCULATIONAHA.125.074752.

Genome and transcriptome-wide analyses identify multiple candidate genes and a significant polygenic contribution in bicuspid aortic valve

A full list of authors and affiliations appears at the end of the article.

Abstract

Background: Bicuspid aortic valve (BAV) is a frequent congenital heart defect with a high heritability. Despite this, only a limited number of genes have been associated with the disease and the molecular mechanisms remain unexplained in most cases. This study aimed to further understand the genetic architecture of BAV.

Methods: A genome-wide association study meta-analysis including 9,631 cases among 65,677 participants was performed. Genes were prioritized using transcriptomic analyses based on RNA sequencing in relevant tissues, including human foetal and adult aortic valves. The impact of the knockdown and/or knockout of four candidate genes on cardiac development was verified in zebrafish. A polygenic risk score was developed and its association with BAV was evaluated in an independent cohort while its association with a wide range of phenotypes (n=976) was evaluated in UK Biobank (n=355,618 individuals).

Results: Thirty-six genomic loci were identified, including 32 that were not described previously. Among the prioritized genes, *KANK2* and *ERBB4* were identified as potentially causal through transcriptomic analyses, colocalization and Mendelian randomization based on gene expression in human aortic valves (n=484), while *PRDM6* and *STRN* were prioritized using similar analyses from aortic (n=326) and left ventricular tissues (n=326), respectively. Targeting four candidate genes (*WNT4*, *LEF1*, *STRN* and *KANK2*) in zebrafish led to disruption in cardiac development. A polygenic risk score was associated with an odds ratio of 2.07 (95% CI 1.90 – 2.25, $P=5.43 \times 10^{-62}$) per standard deviation for BAV and significantly associated with thoracic aortic aneurysm and atrial fibrillation in UK Biobank.

Conclusions: This study supports a significant polygenic contribution to BAV, where the combination of multiple common variants in genes involved in heart morphogenesis disrupts aortic valve development.

Correspondence to: Simon Body, MBChB, MPH, 750 Albany St, Boston, MA 02118, scbody@bu.edu; Sébastien Thériault, MD, MSc, 2725 chemin Sainte-Foy, Quebec City (Quebec), Canada, G1V 4G5, sebastien.theriault@criucpq.ulaval.ca.

*These authors contributed equally.

†These authors jointly supervised this work.

Disclosures

Dr. Krane is a physician proctor and a member of the medical advisory board for Japanese Organization for Medical Device Development (JOMDD), a physician proctor for Peter Duschek, is a medical consultant for EVOTEC and Moderna and has received speakers' honoraria from Edwards, AtriCure, Medtronic and Terumo.

Keywords

Bicuspid aortic valve; Genome-wide association study; Polygenic risk score; RNA sequencing; Zebrafish

Introduction

Bicuspid aortic valve (BAV) is the most frequent congenital heart disease, affecting between 0.5 and 1% of the population^{1,2}. BAV is often accompanied by large vessels and/or other heart defects such as aortopathy (aortic coarctation, dilatation or dissection), hypoplastic left heart syndrome, ventricular and atrial septal defects³. It is associated with a significantly increased risk of calcific aortic valve stenosis (CAVS), a condition with a high risk of death and heart failure, as well as aortic valve insufficiency. It is estimated that two thirds of patients with BAV will eventually develop CAVS while only 15% have a normally functioning valve in the fifth decade⁴.

BAV has a strong genetic component, with a heritability estimated as high as 89%⁵. A prevalence of 7.3% has been reported in individuals with a first-degree relative with BAV in a recent meta-analysis⁶. The transmission of BAV is generally considered as autosomal dominant with incomplete penetrance and variable expressivity⁷. Certain genetic syndromes are associated with a high prevalence of BAV and rare mutations in genes mostly involved in cardiac development have been identified in family studies⁷⁻⁹. However, despite evidence for a clear genetic role in BAV, the identified mutations only explain a minority of BAV cases in sequencing studies¹⁰⁻¹². Most cases of BAV are thought to be caused by complex interactions between multiple genes. Recent genome-wide association studies (GWAS) for BAV have suggested a polygenic contribution to the disease^{13,14}. Common variants located near *GATA4*, *PALMD* and *TEX41* have been associated with BAV^{14,15}. The latest GWAS, including 2,236 BAV cases and 11,604 controls, led to the identification of a fourth locus implicating the *MUC4* gene¹³.

Elucidating the molecular mechanisms responsible for BAV has the potential to improve our understanding of this frequent condition and has implications for screening as well as clinical management. In this study, we report the largest GWAS meta-analysis to date for BAV, including 9,631 cases among 65,677 participants, and identify 32 novel genomic loci. We performed integrative analyses leveraging human aortic valve transcriptome data to prioritize several candidate causal genes and validated the implication of four novel genes during zebrafish cardiac development. We also show a significant polygenic etiology of BAV and report the first polygenic risk score (PRS) robustly associated with the disease.

Methods

Summary statistics of the meta-analysis are available in the NHGRI-EBI GWAS catalog under accession number GCST90707263. The RNA sequencing data from the 484 human aortic valves have been deposited in dbGaP under accession code phs003541.v1.p1. The GTEx project v8 data used in this study are available through dbGaP: <https://gtexportal.org/home/protectedDataAccess>. The adult and foetal aortic valve gene expression

data are available in GEO under accession number GSE282030. Access to individual data from All of Us (<https://allofus.nih.gov/>), UK Biobank (<https://www.ukbiobank.ac.uk/>) and CARTaGENE (<https://cartagene.qc.ca>) is available for registered researchers following the respective application process. GWAS summary statistics from FinnGen are available at <https://www.finnngen.fi/>. The manuscript conforms to the STROBE guidelines.

Study populations

Participants were recruited as part of 17 studies in Europe and North America (Supplemental Methods). The diagnosis of BAV was established using review of medical records, cardiovascular imaging, or direct visualization of the aortic valve during surgery. DNA was extracted from a blood or saliva sample. All phenotype and genotype data were collected following informed consent obtained from all participants and the study was approved by the respective institutional review boards (Supplemental Methods).

Genetic association analyses

DNA genotyping was performed at 8 different sites using microarrays (Table S1). A total of 11 association analyses between BAV cases and matched controls were performed. Quality control procedures included the removal of variants with low call rate, deviating from Hardy-Weinberg equilibrium or with low minor allele frequency and samples with low call rate, high heterozygosity rate, sex discrepancy or non-European ancestry (established using principal component analysis of genotyping data). Phasing and imputation were performed, with TOPMed version r2, Haplotype Reference Consortium version 1.1, UK10K or 1000 Genomes phase 3 as reference. Association analysis was performed with SAIGE or firth logistic regression, adjusting for four to ten ancestry-derived principal components and study-specific covariables (Table S1). The summary statistics from each site were examined centrally for further quality control (Supplemental Methods). A fixed-effect meta-analysis was performed with METAL¹⁶ using inverse-variance weighting. Only variants present in at least two cohorts were considered. The genome-wide significance level was set at $P < 5.0 \times 10^{-8}$. Heterogeneity was evaluated using the Cochran's Q-test. A random-effects meta-analysis was performed as a sensitivity analysis. We verified the association of the lead variant at each genome-wide significant locus in individuals of European ancestry from three large population cohorts: FinnGen, All of Us, and UK Biobank (Supplemental Methods). We then evaluated the association of the lead variants with common BAV complications, namely aortic valve stenosis and thoracic aortic aneurysm, using results from recent GWAS meta-analyses^{17,18}.

Heritability

The phenotypic variance explained by SNPs (SNP heritability) was calculated using LD-score regression¹⁹. Heritability was transformed in the liability scale using a population prevalence of 1% (Supplemental Methods).

Variant annotation and gene mapping

ANNOVAR²⁰ was used to perform variant annotation. Enrichment for functional consequences was calculated using Fisher's exact test from variants in linkage

disequilibrium (LD) with independent significant variants ($r^2 < 0.6$), using 1000 Genomes phase 3 European as reference panel. Missense variants with $P < 1 \times 10^{-5}$ were retrieved to identify variants in high LD ($r^2 > 0.8$) with one of the lead SNPs. CAVIAR²¹ (assuming a single causal variant) and SuSiE²² were used to determine 95% credible sets of genetic variants for each genomic locus.

Expression quantitative trait loci (eQTL)

We have previously generated transcriptomic data from human aortic valve samples from 484 individuals¹⁷. Among the bicuspid valves (n=211), 81.8% had severe stenosis and 25.1% had regurgitation grade 3 or 4, compared to 82.5% and 37.5% for the diseased tricuspid valves (n=215). An additional 58 healthy tricuspid aortic valves were collected from heart transplant receivers (Table S2). All individuals were of European ancestry, established from self-report and principal component analysis from genotypes. Briefly, RNA sequencing was performed on a NovaSeq 6000 instrument (Illumina), aiming for >50 million paired reads per sample. We calculated eQTL for genetic variants located 1 megabase (Mb) up- and downstream of the transcription start site of the genes located on chromosome 1 to 22 (cis-eQTL). Further details on the analysis can be found in the Supplemental Methods. We also retrieved significant eQTLs in 43 non sex-specific tissues from the Genotype-Tissue Expression (GTEx) project v8²³.

Transcriptome-wide association study (TWAS)

Effects of genetic variants on gene expression in the aortic valve were combined with the GWAS meta-analysis results to perform a TWAS. Gene expression models were developed using the PredictDB pipeline²⁴ and the TWAS was performed with the S-PrediXcan extension²⁵ in MetaXcan version 0.7.4. Elastic-net models were trained using nested cross validation from genotype and gene expression adjusted for age, sex, smoking, 60 Probabilistic Estimation of Expression Residuals (PEER) factors²⁶ and the first five ancestry-based principal components. Variants located in a window of ± 1 Mb of the gene of interest were selected. The statistical significance threshold was set at a false discovery rate (FDR) <5%. The same method was used to perform TWAS in three other tissues from GTEx v8: aorta (n=326), heart left ventricle (n=326) and right atrial appendage (n=313). These tissues were selected for their proximity with the aortic valve and considering that BAV is often accompanied by aortopathy and/or congenital heart defects.

Bayesian colocalization and Mendelian randomization (MR)

Colocalization between eQTL and BAV risk was evaluated using COLOC for the genes identified by TWAS²⁷. Variants located within 1 Mb of the gene were considered. A posterior probability of shared signal (PP4) >0.75 was selected to identify a high probability of colocalization. MR was used to evaluate the causal effect of the changes in gene expression level (exposure) on BAV (outcome). Further details on the analysis can be found in the Supplemental Methods.

Selection of candidate genes

We generated a list of candidate genes at each genome-wide associated locus based on variant annotation and gene expression in relevant tissues. More precisely, nearest protein-coding genes to the lead GWAS SNPs, genes with a missense variant in LD ($r^2 \geq 0.8$) with a lead GWAS SNP, genes prioritized by the combined SNP-to-gene strategy (cS2G)²⁸ with a high probability (≥ 0.6), genes that were significant eQTL for a lead GWAS SNP in the aortic valve, aorta, left ventricle or right atrial appendage, and genes significant in the TWAS analysis in the aortic valve, aorta, left ventricle or right atrial appendage were selected. For eQTL and TWAS, only the strongest genes at the locus for the aortic valve or the other tissues were included if not already included in the list.

Pathway enrichment

We used Metascape²⁹ to identify enriched terms in Gene Ontology biological processes, KEGG pathways, Reactome gene sets, canonical pathways, and WikiPathways for the list of candidate genes. Terms were reported when there was a minimum of five overlapping genes and a hypergeometric test was significant using a threshold of $P < 0.001$. Terms with a q-value < 0.05 corresponding to a FDR $< 5\%$ are highlighted.

Foetal aortic valve expression

Human embryos and fetuses included in this study were obtained from voluntary abortions, with age ranging from 9 to 13 post-conception weeks (PCW) (Table S3). Specimen were anonymously donated to research after informed written consent from donors in concordance with French legislation and with prior approval of the protocol (to S.Z.) from the “Agence de la biomédecine” (N° PFS14-011). Human aortic valves at 20 PCW were obtained from medically terminated pregnancies after parents provided their written informed consent to participate in this study (Table S3). The human foetal aortic valves were recognized by their anatomical landmarks. Under the microscope the aortic valve leaflets of 8 foetus hearts at the 9 PCW, 13 PCW, and 20 PCW were isolated with minimal aortic wall contamination and immediately flash frozen in liquid nitrogen. Adult aortic valves were obtained at autopsy of individuals without cardiac problems who suffered a traumatic death (n=3) (Table S4). The investigation conformed to the principles outlined in the Declaration of Helsinki. Following extraction and library preparation, total RNA was sequenced using the Illumina HiSeq 2500 as 50bp single-end reads. The TPM values for the candidate genes were compared between foetal (n=8) and adult aortic valve tissue (n=3) using a two-tailed, unpaired t-test. Further details on the analysis can be found in the Supplemental Methods.

Prioritization of candidate genes from selected features

To prioritize candidate protein-coding genes at the genome-wide significant loci, we assessed a combination of nine features from different sources. We used the following criteria: (1) nearest protein-coding gene to the lead GWAS SNP; (2) the lead GWAS SNP is in LD ($r^2 \geq 0.8$) with a missense variant for the gene; (3) the gene is prioritized by cS2G with a high probability (≥ 0.6); (4) the lead GWAS SNP is a significant eQTL for the gene in the aortic valve or in the aorta, left ventricle or right atrial appendage; (5) the gene is significant in the TWAS analysis in the aortic valve or in the aorta, left ventricle or right

atrial appendage; (6) there is evidence of colocalization (PP4 = 0.75) in the aortic valve or in the aorta, left ventricle or right atrial appendage; (7) there is evidence of causality between gene expression and BAV using MR ($P_{IVW} < 0.05$, $P_{WM} < 0.05$ and $P_{Het} > 0.01$) in the aortic valve or in the aorta, left ventricle or right atrial appendage; (8) the gene has different expression in foetal compared to adult aortic valve ($P_{FDR} < 0.05$); (9) the gene was previously associated with a monogenic condition involving the heart or great vessels in the Online Mendelian Inheritance in Man (OMIM) catalog.

Zebrafish husbandry, generation of morphants and crispants, imaging

Zebrafish were maintained under standardized conditions according to FELASA guidelines³⁰ and experiments were conducted in accordance with the European Communities Council directive 2010/63. The experiments were also performed in compliance with French or German and Brandenburg state law, and carefully monitored by the local authority for animal protection. We followed the ARRIVE and GV-SOLAS guidelines for research involving animals and regarding the 3R principles for experimental animal use. The wild-type AB zebrafish line (WT) was used for live imaging experiments and the *Tg(fli1a:NLS-mCherry)^{ubs10}* line was used for confocal imaging of fixed specimens. Morpholino oligonucleotides (MOs) were obtained from Gene Tools (Philomath, OR, USA) and injected into one-cell stage embryos. Crispants were obtained by co-injecting two or three non-overlapping gRNAs targeting either *lef1*, *wnt4a*, *wnt4b*, *kank2* or *strn* with Cas9 protein into one-cell stage embryos. All gRNAs were prepared and the RNP complexes were assembled as described previously³¹. The sequences of the injected MOs and gRNAs as well as the steps to confirm knockout efficacy are available in the Supplemental Methods. All primers are listed in Table S5. Outflow tract (OFT) valve live imaging, immunostainings, and confocal imaging were performed to characterize the knockdown and knockout models. Further details on the analysis can be found in the Supplemental Methods.

Polygenic risk score (PRS) and phenome-wide association study

We developed PRS using the LDpred2-auto algorithm³². First, to evaluate the performance of a PRS to identify BAV, we ran the GWAS meta-analysis after excluding the QUEBEC-BAV / CARTaGENE cohort, selected as the validation cohort. Second, in order to perform a phenome-wide association study, we used the summary statistics obtained from the complete GWAS meta-analysis to generate a second PRS using LDpred2 as described above. We evaluated the association between this second PRS and 976 selected phenotypes in UK Biobank (Table S6). The analyses in UK Biobank were conducted under data application number 25205.

Statistical analysis

Analyses were performed using R version 4.4.3 unless otherwise specified. Additional details are available in the Supplemental Methods.

Results

Identification of BAV genomic loci

We performed a GWAS meta-analysis including 9,631 BAV cases and 56,046 controls of European ancestry from 17 studies in Europe and North America, combined into 11 case-control association analyses (Supplemental Methods and Table S7). A total of 9,700,115 variants passed the quality control process. The genomic inflation factor was 1.066 and the LD score regression intercept was 1.029. Thirty-six loci reached genome-wide significance ($P < 5 \times 10^{-8}$), including the four loci reported in previous GWAS (near the genes *GATA4*, *PALMD*, *TEX41*, and *MUC4*) (Table 1 and Figure 1). There were 32 novel loci not previously associated with BAV. Among these, three loci had prior association with CAVS, located near *ACTR2*, *TMEM44* and *LPA*¹⁷, and two loci had prior association with ascending thoracic aorta diameter, near *PRDM6* and *FGF9*¹⁸ (Table S8). As a sensitivity analysis, we performed the meta-analysis using random effects, which yielded similar results (Table S9). In a replication meta-analysis from FinnGen, All of Us and UK Biobank (n=4321 cases and 1,085,665 controls), all the 36 lead variants had the same direction of effect and 30 (27 novel) were associated at a nominal threshold ($P < 0.05$) (Table S10). The SNP heritability (phenotypic variance explained by SNPs) was estimated at 11.7% (standard error=1.4%) on the liability scale.

Variant annotation and prioritization

There was a significant enrichment for exonic variants among the variants in linkage disequilibrium with independent significant SNPs (Fisher's exact test, $P = 0.0015$). Missense variants in *MUC4* (rs2246901) and *APOBEC4* (rs1174658) were in high LD ($r^2 = 0.8$) with a lead SNP (Table S11). The 95% credible sets identified using CAVIAR (assuming a single causal variant) and SuSiE are reported for each locus in Table S12. For 12 loci (nearest genes: *WNT4*, *PALMD*, *RCS1*, *SLC8A1*, *ZEB2*, *TMEM44*, *MYLK4*, *LPA*, *DEFB136*, *ADAMTSL1*, *SS18*, *ARFGAP3*), some of the credible sets contained fewer than five variants.

Expression quantitative trait loci

Among the 36 meta-analysis lead SNPs, 25 significant expression quantitative trait loci (eQTL) were identified in the aortic valve, located in 18 loci (Table S13). In the Genotype-Tissue Expression (GTEx) project, 48 significant eQTLs were found in 17 loci, including 6 additional loci with no eQTL in the aortic valve (Table S14). Fibroblasts, atrial appendage, and aorta were among the tissues with the highest number of significant SNP-gene pairs, with 15, 14, and 12, respectively. Taken together, the most significant eQTL was in the aortic valve for 12 loci, including eight genes for which the eQTL was only found in the aortic valve (absent from 43 other tissues in GTEx): *WNT4*, *PALMD*, *ERBB4*, *LEF1*, *LIFR*, *LINC01600*, *VTA1* and *FGF9*. For 12 other loci, the most significant eQTL was found in a GTEx tissue (distributed among nine tissues). These associations include *STRN* and *ATP13A3* in the left ventricle, and *MGST2* and *PRDM6* in the aorta.

Transcriptome-wide association studies, colocalization and Mendelian randomization

To identify relevant genes, we performed a transcriptome-wide association study leveraging expression data from 484 human aortic valves. Genetically-predicted expression levels of 27 genes were significantly associated with BAV ($P_{FDR}<0.05$) (Table S15). Among these, 13 had a high probability of colocalization (posterior probability of shared signal [PP4] >0.75), of which five had supportive evidence of causality from Mendelian randomization analyses, including three located in genome-wide significant loci: *ATP13A3* (previously associated with CAVS¹⁷), *KANK2* and *ERBB4* (Figure 2), and two in other loci: *FES* and *CSK* (Table S15).

The same analyses in relevant tissues from GTEx (aorta and heart tissues) replicated the results for *ATP13A3* (aorta) and *FES* (aorta) and identified other candidate causal genes in genome-wide significant loci: *PRDM6* (aorta) and *STRN* (left ventricle) (Figure 2), and in one other locus: *NNT* (right atrial appendage) (Table S16).

Identification of candidate genes

To select candidate genes at each genome-wide significant locus, we used evidence from variants location and annotation, combined SNP-to-gene strategy, TWAS, colocalization and MR in the aortic valve, aorta and heart tissues. A total of 55 genes were identified, ranging from one to three genes per locus (Table S17).

Pathway enrichment

A pathway enrichment analysis using Metascape was performed from the 55 candidate selected genes (Table S18). The enriched terms ($P_{FDR}<0.05$) included enzyme-linked receptor protein signaling pathway, tube morphogenesis, and heart development. Glial cell differentiation, calcium signaling pathway, cell population proliferation and regulation of actin filament-based process also showed enrichment using a less stringent threshold ($P<0.001$) (Figure 3). Genes associated with terms related to developmental processes included *LEF1*, *WNT4*, *ERBB4* and *PRDM6*.

Foetal aortic valve expression

Gene expression of the 55 candidate genes was compared between human foetal (at 9, 13 and 20 post-conception weeks, $n=8$) and normal adult aortic valve tissues ($n=3$). The expression of 29 genes was significantly different in foetal tissues ($P_{FDR}<0.05$), including *ATP13A3*, *DPF3*, *LEF1*, *PALLD*, *PRDM6*, *RCS1*, *RPS23*, *SLC8A1*, *STRN*, *SUB1*, *TBX3* and *VTA1* with higher expression, suggesting their involvement in aortic valve development (Figure S1).

Association with monogenic conditions

Among the 55 candidate genes, seven were previously associated with a monogenic form of a cardiovascular condition, including *PRDM6* (patent ductus arteriosus) and *ATP13A3* (pulmonary hypertension) (Table S17). Of note, only *GATA4* was previously reported in a sequencing study in familial cases of BAV³³.

Prioritization of candidate genes

To prioritize the candidate genes, we summarized the evidence from different sources using nine features based on variant location, annotation, gene expression in relevant tissues and association with a monogenic condition. Taken together, 13 genes located at genome-wide significant loci had five or more features suggesting their implication in BAV (Figure 4 and Table S17). The ten genes with the most features were *PRDM6*, *ATP13A3*, *ERBB4*, *STRN*, *ARPC5*, *KANK2*, *LEF1*, *MUC4*, *RBM38*, and *SLC8A1*. Overall, bioinformatics analyses supported by gene expression data from adult and foetal aortic valves prioritized several candidate genes, many of them involved in cardiac morphogenesis.

Functional experiments reveal an involvement of several candidate genes in zebrafish cardiac development

In order to validate candidate genes by functional analyses, we selected the zebrafish model and focussed on the cardiac outflow tract (OFT) valve, which is related to the aortic valve in higher vertebrates and humans (Figure 5A-C)^{34,35}. We selected candidate genes identified at GWAS loci with an association between a lower predicted expression in the aortic valve or other heart tissues and BAV risk. These included *LEF1* and *WNT4*, two components of the canonical WNT signaling pathway previously implicated in cardiac valvulogenesis^{36,37}. In addition, we selected *STRN* and *KANK2*, two genes with several features suggesting a possible association with BAV (Figure 4), but which have not been previously implicated in valvulogenesis. The zebrafish genome harbors two *WNT4* paralogues, *wnt4a* and *wnt4b*, and a single orthologous gene for *lef1*, *strn*, and *kank2*.

First, we used a CRISPR/Cas9-mediated knockout approach to target the genomic loci of the five selected zebrafish genes. The embryonic “crispant” phenotypes of *lef1*, *wnt4a* and *wnt4b* were severe and included cardiac edema, which precluded the analysis of cardiac valves (Figure S2). To overcome this difficulty and to visualize OFT valve development, we switched to an antisense morpholino oligonucleotides (MO)-based knockdown approach, targeting the translational start (ATG-MO) for these three genes and titrated the MOs to identify a concentration which did not induce any gross developmental phenotypes. Subsequently, we imaged the valve at 7 days post-fertilization (dpf) using two-photon microscopy. In wild-type (WT) and standard control MO (Gene Tools), the OFT valve developed normally with two defined valve leaflets (Figure 5B, F). In comparison, the OFT valves in nearly 80% of *lef1* morphants were highly dysmorphic, enlarged and misshapen compared with the WT ($P < 0.0001$, Figure 5D, F). Among *wnt4a* or *wnt4b* morphants, approximately 25% displayed dysmorphic OFT valve leaflets and this proportion increased to nearly 60% in *wnt4a/wnt4b* double morphants ($P = 0.0003$, Figure 5E, F). These results indicate that a loss of *lef1* or *wnt4* results in defective OFT valve development. Moreover, we designed a second set of MOs, targeting exon-intron splice sites (splMO) of *lef1*, *wnt4a* or *wnt4b* which allowed us to establish that RNA transcription had been disrupted by RT-PCR (Figure S3). As for the ATG-MO, *lef1* and *wnt4a/wnt4b* splMO injections resulted in significant dysmorphic valve development, which provides further evidence that these genes are required for normal aortic valve development ($P = 0.0004$ and $P < 0.0001$ respectively, Figure S3).

The other two candidate genes (*strn*, *kank2*) were analyzed by CRISPR/Cas9-mediated knockout using pairs of gRNAs flanking parts of the coding regions to induce genomic deletions (Figure S4A, B). Quantitative PCR confirmed significantly reduced expression of both *strn* and *kank2* in injected embryos (Figure S4C).

Live imaging of the OFT valve at 7 dpf using two-photon microscopy revealed that 40% (n = 6/15) of *strn* crispants exhibited dysmorphic valve leaflets ($P=0.0068$, Figure 5G, I), while no obvious valve defects were observed in *kank2* crispants ($P=0.48$, Figure 5H, I) or with control crispants ($P>0.9999$, Figure 5I). These live imaging experiments and qPCR, described above, were performed on injected embryos without prior genotyping, as genotyping requires sacrificing the embryos and is thus incompatible with live imaging and RNA extraction.

To assess genome editing efficacy, PCR was used to detect genomic deletions in a separate set of embryos. We defined complete deletion as the presence of a deletion-specific band and absence of the wild-type band (Figure S4A', B'). Complete deletions were detected in 20.5% of embryos for *strn* (n = 8/39) and 36.4% for *kank2* (n = 12/33).

To further elucidate whether a loss of *strn* or *kank2* may cause more subtle defects in valvulogenesis, we performed whole-mount immunohistochemistry on crispants with complete deletions at 5 dpf that were generated in a *Tg(fli1a:NLS-mCherry)^{ubs10}* transgenic background marking endothelial cells. Additional labeling against Alcam to mark endothelial cells contributing to the valve leaflets and myocardial cell membranes and against DAF-FMDA to mark vascular smooth muscle cells was performed. At 5 dpf, the WT OFT region is characterized by a thickened layer of smooth muscle cells surrounding the endothelium, with a characteristic two-leafed structure formed by OFT valve endothelial cells that can be identified based on Alcam expression (Figure 5C; Figure S4D). Careful inspection of these valvular structures in crispants (n=9 for *strn*; n=9 for *kank2*) did not reveal any abnormalities (Figure S4E, F). Next, we used three-dimensional reconstructions of confocal microscopic z-stack recordings for morphometric measurements of the entire OFT region, which revealed that *strn* crispants, but no *kank2* crispants, had a significantly shortened OFT length ($P=0.044$) and reduced OFT length/width ratio ($P=0.046$) (Figure S4G). This suggested an involvement of *strn* in OFT morphogenesis. Since other morphometric measurements of this region were not significantly altered, *kank2* is apparently dispensable for correct OFT formation in zebrafish.

To assess whether *strn* or *kank2* have any role in the development of the valve at the atrioventricular canal (AVC) separating the atrium and the ventricle, we characterized its development at 60 hours post-fertilization (hpf). At this stage, some AVC endocardial cells have ingressed into the cardiac jelly separating the endocardium and myocardium and have formed a multi-layered leaflet structure (Figure S4H)³⁸. High-resolution confocal microscopic z-stack recordings did not reveal any gross abnormalities in AVC valve morphogenesis in *strn* (n=10 crispants analyzed) or *kank2* crispants (n=10 crispants analyzed) (Figure S4I, J). Yet, quantifications of Alcam⁺ endocardial cells revealed a significantly increased cell count ($P=0.0034$) in *kank2* crispants compared with WT or *strn* crispants (analysis based on n=4 WT embryos, n=10 *kank2* crispants, n=10 *strn* crispants)

(Figure S4K). Taken together, these analyses provide functional evidence for a potential involvement of several candidate genes identified from the BAV GWAS meta-analysis in zebrafish cardiac valvulogenesis.

Polygenic risk score

In order to support the polygenic nature of BAV and estimate the potential value for risk prediction, we developed a PRS using LDpred2 in a subset of cohorts (n=8,853 cases and 50,600 controls) and evaluated its performance in the QUEBEC-BAV / CARTaGENE cohort (n=778 cases and 5,446 controls). Each standard deviation increase (SD) of the PRS was associated with an odds ratio (OR) of 2.07 (95% CI 1.90 – 2.25, $P=5.43 \times 10^{-62}$) for BAV. A PRS above the 90th percentile was associated with an OR of 3.39 (95% CI 2.83 – 4.06) (Figure 6A). The area under the receiver operating characteristic curve (AUC) was 0.692 (95% CI 0.673 – 0.711) (Figure 6B). We then created a second PRS using the complete meta-analysis summary statistics and evaluated its association with 976 phenotypes in UK Biobank. As expected, there was a significant association with surgical intervention to the aortic valve (OR=1.52 per SD, 95% CI 1.46 - 1.59, $P=1.91 \times 10^{-84}$), aortic valve stenosis (OR=1.34 per SD, 95% CI 1.30 - 1.38, $P=3.72 \times 10^{-73}$) and aortic valve insufficiency (OR=1.19 per SD, 95% CI 1.13 - 1.25, $P=4.13 \times 10^{-11}$), but also with thoracic aortic aneurysm (OR=1.26 per SD, 95% CI 1.18 - 1.36, $P=1.45 \times 10^{-10}$) and atrial fibrillation/flutter (OR=1.03 per SD, 95% CI 1.02 - 1.05, $P=9.10 \times 10^{-7}$) (Figure 6C and Table S6). These findings support a polygenic contribution to BAV and some of its comorbidities.

Discussion

Through a GWAS meta-analysis including 9,631 BAV cases, we identified 36 genome-wide significant loci, including 32 reported for the first time, 27 of which had evidence of association in a replication analysis supporting the robustness of the findings. We prioritized several candidate causal genes using multiple approaches based on extensive transcriptomic data in human aortic valves and functional experiments in zebrafish. We also show a significant polygenic contribution to BAV by deriving a first PRS robustly associated with this condition.

Among the novel genomic risk loci, two genes, *KANK2* and *ERBB4*, were identified as potentially causal through eQTL, colocalization and Mendelian randomization analyses based on expression in human aortic valves. *KANK2* codes for KN motif and ankyrin repeat domains 2, a regulator of actin polymerization with a negative effect on cell migration through modulation of integrin activity³⁹. It is one of several actin regulatory genes identified in the study (e.g., *ACTR2*, *ARPC5*), suggesting an important role of this molecule in aortic valve development. We show that genetically-predicted lower expression of *KANK2* in human aortic valves is associated with BAV. Although we did not observe major anomalies in heart or valve morphology in the molecular knockout zebrafish model, there was a significant increase in endocardial cells at 60 hpf, consistent with a potential role in cell migration during the development of aortic valve leaflets. *ERBB4* codes for erb-b2 receptor tyrosine kinase 4, a membrane protein activated by neuregulins involved in cardiac embryonic development and valvulogenesis^{40,41}. Evidence of reduction in the size of the

endocardial cushion and absence of ventricular trabeculae was previously observed during embryogenesis in a mouse *ErbB4* knockout model⁴². Our findings that *ERBB4* expression in human aortic valve is inversely related to BAV are coherent with a role of this gene in aortic valve development. Another gene prioritized at a genomic locus, *ATP13A3*, was recently identified in a TWAS for CAVS¹⁷ and previously associated with a monogenic form of pulmonary artery hypertension⁴³.

Other genes were prioritized through transcriptomic analyses in relevant tissues, including *STRN* and *PRDM6*. *STRN* encodes striatin, a component of the STRIPAK complex mediating various signaling pathways and implicated in actin cytoskeleton organization and cell adhesion^{44,45}. This locus was previously associated with heart failure; the lead variant for BAV, rs62132550, is in high linkage disequilibrium ($r^2=0.938$) with the lead variant identified for heart failure, rs7605601 (same direction of effect)⁴⁶. A heterozygous knockout mouse model showed inhibition of cardiomyocyte hypertrophy following angiotensin II stimulation, suggesting a role in cardiac remodelling⁴⁷. We show that *STRN* expression is notably higher in foetal compared to adult aortic valve tissue and that lower genetically-predicted expression in the heart left ventricle is associated with BAV. The zebrafish molecular knockout model showed OFT valve defects at 7 dpf and a reduction in the OFT length at 5 dpf, consistent with a role of this gene in cardiac development. *PRDM6* codes for PR/SET domain 6, a transcriptional repressor involved in the epigenetic regulation of vascular smooth muscle cells (VSMC) contractile proteins⁴⁸. It is highly expressed in the cardiac OFT and loss-of-function variants in the gene have been associated with patent ductus arteriosus, possibly through decreased VSMC proliferation and contractility^{49,50}. We observed an increased expression of *PRDM6* in human foetal compared to adult aortic valve tissue. *PRDM6* was previously associated with thoracic aortic aneurysm by TWAS based on genetically-predicted expression in the aorta (positive association)⁵¹; we now show a similar association for BAV.

Several of the prioritized genes were related to Wnt signaling, a highly conserved developmental pathway involved in organogenesis, including heart valvulogenesis^{37,52}. We report evidence for a role in BAV of two important genes in this pathway located at genome-wide significant loci, *LEF1* and *WNT4*. Notably, the lead variants at these two loci were negative eQTL only found in the aortic valve. *LEF1* encodes lymphoid enhancer binding factor 1, a transcription factor acting as a nuclear effector after binding with β -catenin, an important intracellular mediator in the canonical Wnt signaling pathway⁵³. This gene was shown to be expressed specifically in endocardial cushions and forming valve cusps during mouse embryogenesis^{37,54}. *WNT4* is a member of the Wnt family shown to be expressed specifically in endocardial endothelial cells overlying the atrioventricular and OFT cushions in mice embryos, with a potential role in endocardial-to-mesenchymal transformation^{37,54}. In zebrafish, a CRISPR/Cas9-mediated knockout of these genes (*lef1*, *wnt4a* or *wnt4b*) caused severe cardiac edema while knockdown using morpholinos led to dysmorphic OFT valve leaflets at 7 dpf in several individuals, with a higher proportion in the double knockdown of *wnt4a* and *wnt4b* compared to single gene knockdown, corroborating the role of these genes in OFT development.

Evidence of the causal implication of three other genes located outside of a genome-wide significant locus was observed in the transcriptomic analyses. *CSK*, coding for C-terminal Src kinase, phosphorylates multiple substrates and has an important role in angiogenesis. Increase in CSK activity in endothelial cells was shown to induce vascular malformations and ballooning in a 3D model⁵⁵. The lead variant in the meta-analysis is also strongly associated with diastolic and systolic blood pressure as well as arteriolar tortuosity in the retina^{56,57}. In our study, an increase in *CSK* genetically-predicted expression in the aortic valve was associated with BAV. Genetically-predicted expression in the right atrial appendage of *NNT*, coding for nicotinamide nucleotide transhydrogenase, a mitochondrial protein, was also positively associated with BAV. Pathogenic mutations in *NNT* have been identified in individuals with left ventricular noncompaction. In the same study, injection of morpholinos targeting orthologous genes in zebrafish caused cardiac edema and contractile dysfunction, which was attributed to aberrant cardiomyocyte proliferation during heart development⁵⁸. We also found a negative association between genetically-predicted expression of *FES* in the aortic valve and aorta and BAV. This gene was previously identified in a similar analysis for CAVS¹⁷ and has been associated with coronary artery disease⁵⁹ and blood pressure⁵⁶.

Taken together, the majority of the genomic risk loci identified for BAV were not previously associated with valvular heart diseases or aortic dilation. Some of the loci identified, such as the *LPA* locus, have been associated with CAVS. They could contribute to the development of aortic stenosis in individuals with BAV, as previously suggested⁶⁰. However, it remains possible that some of the loci identified in CAVS GWAS reflect their association with BAV since the valve morphology is often not accurately identified in large biobanks. Another hypothesis is that some loci are associated both with BAV and CAVS on a tricuspid valve, as already reported for *NOTCH1*^{61,62} and *PALMD*^{15,63}. An enrichment of BAV has also been found in first-degree relatives of patients with CAVS with a tricuspid aortic valve, suggesting a complex interplay and a common genetic predisposition between BAV and CAVS⁶⁴. Further studies are needed to understand the biological mechanisms at play.

Among the candidate genes identified, only a few were previously associated with a monogenic condition, of which only *GATA4* had rare variants reported in cases of BAV^{33,65}. These findings suggest that common variants with lower effect sizes in distinct genes are involved in BAV. Overall, the phenotypic variance explained by the evaluated variants was estimated at 11.7%. In addition to the contribution of rare variants, gene-gene and gene-environment interactions could explain part of the missing heritability. We also report for the first time a PRS strongly associated with BAV, implicating a significant polygenic contribution to the development of this congenital heart defect. Each SD of the PRS was associated with an OR of 2.07, which is higher than what has been observed for complex traits, including CAVS^{66,67}. The PRS was also associated with frequent complications of BAV in an independent cohort, including aortic valve stenosis and regurgitation, thoracic aortic aneurysm (encompassing ascending aorta, aortic arch and descending aorta), and atrial fibrillation. Such scores could therefore potentially be used to facilitate early identification of individuals at high risk of BAV and its consequences. Prospective studies are needed to determine the predictive value for the progression of BAV-related diseases.

The study has some limitations. First, several cohorts recruited participants undergoing surgery for aortic valve replacement, which might have led to a bias towards BAV complicated with either aortic stenosis, regurgitation or aortopathy. Second, the analysis was restricted to participants of European ancestry due to a lack of sufficient cases for other ancestries. Incidence has been reported to be lower in African populations⁶⁸, which could explain why we were not able to include a sufficient number of individuals. Analyses including more diverse populations are needed to verify if the results are generalizable and discover other loci that could be specific to other ancestries. Third, further functional studies are needed to clarify the precise role of the identified genes in the development of BAV.

In conclusion, through a comprehensive genomic approach, we identified several novel genes involved in BAV, many of which are related to pathways involved in cardiac embryonic development. Our findings highlight a polygenic origin for BAV, where the combination of several common variants disrupts aortic valve development.

Supplementary Material

Refer to Web version on PubMed Central for supplementary material.

Authors

Sébastien Thériault, MD, MSc^{1,*}, Jacob A. Holdcraft, MA^{2,*}, Dinara Sharipova, MSc^{3,*}, Adèle Faucherre, PhD^{4,*}, Radoslaw M. Debiec, MD, PhD^{5,*}, Gina M. Peloso, PhD^{2,*}, Baravan Al-Kassou, MD⁶, Sary Aranki, MD⁷, Elena Ashikhmina Swan, MD, PhD⁸, Andrea Ballotta, MD⁹, Michele Bellino, MD¹⁰, Hanna M. Björck, PhD^{11,12}, Anne Sophie Boureau, MD, PhD¹³, Peter S. Braund, PhD⁵, François Corriveau, BS¹⁴, François Dagenais, MD¹, Lasse Folkersen, PhD¹⁵, Amalia Forte, PhD¹⁶, Michael D Francke, MD⁷, Alessandro Frigiola, MD¹⁷, Svetlana Gorbato, MPH⁷, Dongchuan Guo, PhD¹⁸, Karam M. Habchi, MD¹⁹, Mahyar Heydarpour, PhD²⁰, Eric M. Isselbacher, MD, MSc²¹, Chris Jopling, PhD⁴, Fabien Laporte, PhD¹³, Solena Le Scouarnec, PhD¹³, Zhonglin Li, MSc¹, Peter Lichtner, PhD²², Carlo Maj, PhD²³, Hasanga D. Manikpurage, PhD¹, Christopher P. Nelson, PhD⁵, Thy B. Nguyen, MD²⁴, Russell A Norris, PhD²⁵, Chin Siang Ong, PhD²⁶, Philippe Pibarot, PhD¹, Tanmoy Roychowdhury, PhD^{27,28}, Berardo Sarubbi, MD²⁹, Floriane Simonet, MSc¹³, Thoralf Sundt, MD²¹, Ida Surakka, PhD²⁷, Idit Tessler, MD, PhD³⁰, Cristen J. Willer, PhD²⁷, Susanne Wittmann, PhD²², Bo Yang, MD, PhD²⁷, Igor Berezovets, MD³¹, Stefanie A. Doppler, MD³², Martina Dreßen, MD³², Katharina Knoll, MD^{33,34}, Thomas Puehler, MD³¹, Heribert Schunkert, MD^{33,34}, Jean-François Avierinos, MD, PhD³⁵, Malenka M. Bissell, MD, PhD³⁶, Aidan P. Bolger, MD, PhD⁵, Yohan Bossé, PhD¹, Eduardo Bossone, MD, PhD³⁷, Maria Brion, PhD³⁸, Rodolfo Citro, MD, PhD^{39,40}, Carlo de Vincentiis, MD¹⁷, G. Michael Deeb, MD⁴¹, Alessandro Della Corte, MD, PhD¹⁶, Christian Dina, PhD¹³, Ronen Durst, MD⁴², Stephan Ensminger, MD³¹, Per Eriksson, PhD^{11,12}, Arturo Evangelista, MD, PhD⁴³, Anders Franco-Cereceda, MD, PhD^{12,44}, Dan Gilon, MD⁴², Betti Giusti, PhD⁴⁵, Simon L. Hetherington, MD⁴⁶, Gordon S. Huggins, MD⁴⁷, Markus Krane, MD^{32,34}, Thierry Le Tourneau, MD, PhD¹³, Giuseppe Limongelli, MD, PhD⁴⁸, Patrick Mathieu, MD,

MSc¹, David Messika-Zeitoun, MD, PhD⁴⁹, Hector I. Michelena, MD⁵⁰, Dianna Milewicz, MD, PhD¹⁸, Jochen D. Muehlschlegel, MD, MMSc, MBA⁵¹, David R. Murdock, MD¹⁸, Georg Nickenig, MD⁶, Stefano Nistri, MD, PhD^{45,52}, Markus M. Nöthen, MD⁵³, Francesca Pluchinotta, MD, PhD¹⁷, Siddharth K Prakash, MD, PhD¹⁸, Nilesh J. Samani, MD⁵, Jean-Jacques Schott, PhD¹³, Tom R. Webb, PhD⁵, Stéphane Zaffran, PhD^{54,†}, Salim Abdelilah-Seyfried, PhD^{3,†}, Kim Eagle, MD^{55,†}, Johannes Schumacher, MD^{23,53,†}, Teresa Trenkwalder, MD^{33,34,†}, Simon Body, MD, MPH^{56,†}

Affiliations

- ¹Institut universitaire de cardiologie et de pneumologie de Québec – Université Laval, Quebec city, Canada.
- ²Department of Biostatistics, Boston University School of Public Health, Boston, USA.
- ³Department of Animal Physiology, Institute of Biochemistry and Biology, University of Potsdam, Potsdam, Germany.
- ⁴IGF, Univ Montpellier, CNRS, Inserm, Montpellier, France.
- ⁵Department of Cardiovascular Sciences, Leicester British Heart Foundation Centre of Research Excellence and NIHR Leicester Biomedical Research Centre, University of Leicester, Leicester, United Kingdom.
- ⁶Department of Medicine II, Heart Center Bonn, University of Bonn and University Hospital Bonn, Bonn, Germany.
- ⁷Brigham and Women's Hospital, Boston, USA.
- ⁸Mayo Clinic, Rochester, USA.
- ⁹Centro Cardiologico Monzino IRCCS Via Parea, 4 Milan University, Milan, Italy.
- ¹⁰University Study of Salerno, Salerno, Italy.
- ¹¹Division of Cardiology, Center for Molecular Medicine, Department of Medicine, Karolinska Institutet, Stockholm, Sweden.
- ¹²Karolinska University Hospital, Solna, Sweden.
- ¹³Nantes Université, CHU Nantes, CNRS, INSERM, l'institut du thorax, Nantes, France.
- ¹⁴Université Laval, Québec, Canada.
- ¹⁵Nucleus Genomics, New York, USA.
- ¹⁶University of Campania L. Vanvitelli, Naples, Italy.
- ¹⁷IRCCS Policlinico San Donato, San Donato Milanese, Italy.
- ¹⁸Department of Internal Medicine, McGovern Medical School, The University of Texas Health Science Center at Houston, Houston, USA.

19. New York-Presbyterian Weill Cornell Medical Center, New York, USA.
20. Department of Medicine, Brigham and Women's Hospital, Boston, USA.
21. Massachusetts General Hospital, Boston, USA.
22. Helmholtz Munich, Neuherberg, Germany.
23. Institute of Human Genetics, Philipps University of Marburg, Marburg, Germany.
24. University of Colorado, Aurora, USA.
25. Medical University of South Carolina, Charleston, USA.
26. Yale University School of Medicine, New Haven, USA.
27. Department of Internal Medicine, Division of Cardiology, University of Michigan, Ann Arbor, USA.
28. Department of Biology & Koita Centre for Digital Health, Trivedi School of Biosciences, Ashoka University, Sonapat, India.
29. Adult Congenital Heart Disease and Congenital and Familial Arrhythmias Unit, Monaldi Hospital, Naples, Italy.
30. Sheba Medical center, Ramat Gan, Israel.
31. Department of Cardiac and Thoracic Vascular Surgery, University Heart Center Lübeck, University Medical Center Schleswig-Holstein, Lübeck, Germany.
32. Department of Cardiovascular Surgery, Institute Insure, German Heart Center Munich, School of Medicine and Health, TUM University Hospital, Technical University of Munich, Munich, Germany.
33. Department of Cardiovascular Diseases, German Heart Centre Munich, School of Medicine and Health, TUM University Hospital, Technical University of Munich, Munich, Germany.
34. German Center for Cardiovascular Disease (DZHK), Partner Site Munich Heart Alliance, Munich, Germany.
35. Service de Cardiologie, AP-HM, Hôpital de la Timone, Marseille, France.
36. Leeds Institute of Cardiovascular and Metabolic Medicine, University of Leeds, Leeds, United Kingdom.
37. Department of Public Health, Faculty of Medicine, University of Naples "Federico II", Naples, Italy.
38. Xenética Cardiovascular, Instituto de Investigación Sanitaria de Santiago, Complejo Hospitalario Universitario de Santiago, Santiago de Compostela, Spain.
39. Department of Medicine and Health Science, University of Molise, Campobasso, Italy.
40. Department of Vascular Pathophysiology, IRCCS Neuromed, Pozzilli, Isernia, Italy.

41. Department of Cardiac Surgery, Michigan Medicine, University of Michigan, Ann Arbor, USA.
42. Cardiology Department, Hadassah Hebrew University Medical Center, Jerusalem, Israel.
43. Hospital Universitari Vall d'Hebron, Barcelona, Spain.
44. Department of Molecular Medicine and Surgery, Karolinska Institutet, Stockholm, Sweden.
45. Department of Experimental and Clinical Medicine, University of Florence, Florence, Italy.
46. Kettering General Hospital NHS Foundation Trust, Kettering, UK.
47. Tufts Medical Center, Boston, USA.
48. Department of Translational Medical Sciences, University of Campania Luigi Vanvitelli, Naples, Italy.
49. Division of Cardiology, University of Ottawa Heart Institute, Ottawa, Canada.
50. Department of Cardiovascular Medicine, Mayo Clinic, Rochester, USA.
51. Department of Anesthesiology and Critical Care Medicine, Johns Hopkins University School of Medicine, Baltimore, USA.
52. CMSR Veneto Medica, Altavilla Vicentina, Italy.
53. Institute of Human Genetics, University of Bonn and University Hospital Bonn, Bonn, Germany.
54. Aix Marseille Université, INSERM, MMG, U1251, Marseille, France.
55. Michigan Medicine, University of Michigan, Ann Arbor, USA.
56. Boston University, Boston, USA.

Acknowledgments

We thank the research team at the cardiac surgical database and biobank of the Institut universitaire de cardiologie et de pneumologie de Québec for their valuable assistance and all the participants. We thank the CARTaGENE study team and participants. We gratefully acknowledge All of Us participants for their contributions, without whom this research would not have been possible. We also thank the National Institutes of Health's All of Us Research Program for making available the participant data examined in this study. We want to acknowledge the participants and investigators of the FinnGen study. We thank all the UK Biobank participants and administration team. We thank Imagerie du Petit Animal de Montpellier (IPAM) and FranceBioImaging. We thank Anne-Marie Séguin, Martina Caiazza, Joana Castillo Di Giacinto, Annapaola Cirillo, Fiorella Fratta, Adelaide Fusco, James Gosnell, Jacqueline Jennings, Federica Lo Presti, Emanuele Monda, Maria Giovanna Russo and Jasmine T. Shahram for their assistance. We would like to acknowledge the contribution of Jeanette Erdmann, who passed away in 2023.

S.T., D.S., A. Faucherre and S.Z. wrote the first draft of the manuscript.

S.T., D.S., A. Faucherre, S.Z., S.A.-S., K.E., J.S., T.T. and S.B. designed the study.

S.T., P.P., J.-F.A., M.M.B., A.P.B., Y.B., M. Brion, A.D.C., S.E., P.E., A.F.-C., B.G., G.S.H., M.K., T.L.T., G.L., P.M., D.M.-Z., H.I.M., D.M., J.D.M., G.N., S.N., M.M.N., S.K.P., N.J.S., J.-J.S., S.Z., S.A.-S., J.S., T.T. and S.B. supervised part of the project.

D.S., A. Faucherre, R.M.D., B.A.-K., E.A.S., H.M.B., K.M.H., M.H., C.J., H.D.M., C.P.N., P.P., I.S., I.B., S.A.D., M.D., K.K., T.P., H.S., A.P.B., M. Brion, R.C., A.D.C., S.E., P.E., A.F.-C., B.G., S.L.H., T.L.T., G.L., P.M., D.M.-Z., H.I.M., D.M., J.D.M., G.N., M.M.N., S.K.P., N.J.S., T.R.W., S.Z., S.A.-S., T.T. and S.B. contributed to data collection.

S.T., J.A.H., D.S., G.M.P., P.S.B., L.F., M.H., F.L., Z.L., C.M., C.S.O., T.R., M. Brion, C.D., D.R.M. and S.A.-S. performed statistical and/or association analyses.

J.A.H., R.M.D., G.M.P., B.A.-K., S.A., E.A.S., A.B., M. Bellino, H.M.B., A.S.B., P.S.B., F.C., F.D., L.F., A. Forte, M.D.F., A. Frigiola, J.G., S.G., D.G., K.M.H., M.H., W.H., E.M.I., C.J., F.L., S.L.S., Z.L., P.L., C.M., H.D.M., T.B.N., R.A.N., C.S.O., P.P., T.R., B.S., F.S., T.S., I.S., I.T., C.J.W., S.W., B.Y., I.B., S.A.D., M.D., K.K., T.P., H.S., J.-F.A., M.M.B., A.P.B., Y.B., E.B., M. Brion, R.C., C.V., G.M.D., A.D.C., C.D., R.M.D., S.E., P.E., A.E., A.F.-C., D.G., B.G., S.L.H., G.S.H., M.K., T.L.T., G.L., P.M., D.M.-Z., H.I.M., D.M., J.D.M., D.R.M., G.N., S.N., M.M.N., F.P., S.K.P., N.J.S., J.-J.S., T.R.W., S.Z., S.A.-S., K.E., J.S., T.T. and S.B. reviewed the manuscript.

Sources of Funding

S.T. was supported by the Canadian Institutes of Health Research (PJT – 162344) and by the Heart and Stroke Foundation of Canada (G-19-0026386). D.S. was supported by the Deutsche Forschungsgemeinschaft (NO246/17-1). A. Faucherre is part of the Laboratory of Excellence Ion Channel Science and Therapeutics supported by a grant from the Agence nationale de la recherche (ANR; ANR-10-INSB-04). R.M.D., A.P.B., and T.R.W. received support from the British Heart Foundation Accelerator Award (AA/18/3/34220). R.M.D., A.P.B., N.J.S., and T.R.W. are supported by a British Heart Foundation Research Excellence Award (RE/24/130031). R.M.D. received support from the Academy of Medical Sciences (Award number RM61G1013/42885). The BRAVE study is supported by the National Institute for Health Research Leicester Biomedical Research Centre. The BRAVE study also received research support from the Heart Link Children's Charity, East Midlands, UK (Charity registration number 1203709). B.A.-K., G.N., M.M.N., and J.S. were supported by the Deutsche Forschungsgemeinschaft (DFG) (TRR259). H.M.B. was supported by the Swedish Research Council and Swedish Heart-Lung Foundation (2020-01442, 2022-0136). F.L. was supported by International Research Program (IRP) - VERACITIES, an initiative under the I-SITE NExT health and engineering program (École Centrale de Nantes & Nantes University). Additional support was provided by Inserm and Centre national de la recherche scientifique (CNRS) through the IRP-GAINES program. P.P. was supported by the Canadian Institutes of Health Research (FDN-143225). M.D. was supported by Förderverein Deutsches Herzzentrum München. H.S. was supported by the framework of DigiMed Bayern (www.digimed-bayern.de; DMB-1805-0001) by the Bavarian State Ministry of Health, Care and Prevention and the Bavarian State Ministry of Science and the Arts through the DHM-MSRM Joint Research Center (1530/891 02), the Leducq Foundation (18CVD02), the German Heart Foundation (Deutsche Herzstiftung e.V.), the German Research Foundation (DFG) as part of the Sonderforschungsbereich SFB 1123 (B02) and the Sonderforschungsbereich SFB TRR 267 (B05), the German Federal Ministry of Economics and Energy in its scheme of ModulMax (Grant No: ZF4590201BA8, the Horizon Europe Framework Programme (HORIZON) by the European Commission (MIRACLE 101115381), the German Federal Ministry of Education and Research (BMBF) within the framework of COMMITMENT (01ZX1904A). The funders of the study had no role in study design, data collection, data analysis, data interpretation, or writing of the manuscript. Y.B. holds a Canada Research Chair in Genomics of Heart and Lung Diseases and was supported by the Canadian Institutes of Health Research and Heart and Stroke Foundation of Canada (MOP – 10248, MOP – 137058, PJT – 153396, PJT – 159641). M. Brion was supported by Instituto de Salud Carlos III (ISCIII) (PI22/00286). A.D.C. was supported by the Italian Ministry of Work, Health and Social Politics (GR-2009-1580434). C.D. was supported by a grant from the Fondation Genavie. P.E. was supported by the Swedish Research Council and Swedish Heart-Lung Foundation (2020-01442, 2021-0521). M.K. was supported by Deutsche Forschungsgemeinschaft (DFG) projects KR3770/7-3, and KR3770/14-1. T.L.T. was supported by Fondation Coeur et Recherche (2012), Fédération Française de Cardiologie (2018). P.M. was supported by the Canadian Institutes of Health Research (PJT-191807). The COFRASA and GENERAC studies (D.M.-Z.) are supported by a grant from Assistance Publique-Hôpitaux de Paris, France. D.M. was supported by ARTIVION. J.D.M. was supported by the NIH (R01HL149998) and by National Heart, Lung, and Blood Institute (NHLBI) (R01HL118266, R01HL150401). S.K.P. was supported by the NHLBI (R01HL137028, R21HL150383). J.J.S. was supported by the French National Research Agency (ANR: [13-BSV6-0011]), the Fondation pour la Recherche Médicale (FRM: [DCV20070409278]), and the International Research Program (IRP) - VERACITIES, an initiative under the I-SITE NExT health and engineering program (École Centrale de Nantes & Nantes University). Additional support was provided by Inserm and CNRS through the IRP-GAINES program. S.Z. was supported by "Association Française contre les Myopathies" [NMH-Decrypt Project], the "Fondation pour la Recherche Médicale" [DPC20111123002], the "Institut National de la Santé et de la Recherche Médicale" and "la Fondation Leducq". S.A.-S. was supported by Deutsche Forschungsgemeinschaft (DFG) projects SE2016/7-3, SE2016/10-1, SE2016/13-1, NO246/17-1, and the Leducq Transatlantic Network of Excellence "21CVD03 - ReVAMP". T.T. was supported by Deutsche Herzstiftung. S.B. was supported by the National Heart, Lung, and Blood Institute (R01HL114823, R21HL150373).

Non-standard Abbreviations and Acronyms

AUC	area under the receiver operating characteristic curve
AVC	atrioventricular canal
BAV	bicuspid aortic valve
CAVS	calcific aortic valve stenosis
cS2G	combined SNP-to-gene
dpf	day post-fertilization
eQTL	expression quantitative trait locus
FDR	false discovery rate
GTE_x	Genotype-Tissue Expression
GWAS	genome-wide association study
hpf	hour post-fertilization
LD	linkage disequilibrium
MAF	minor allele frequency
MOs	morpholino oligonucleotides
MR	Mendelian randomization
OFT	outflow tract
OMIM	Online Mendelian Inheritance in Man
OR	odds ratio
PCW	post-conception week
PP4	posterior probability of shared signal
PRS	polygenic risk score
SD	standard deviation
TWAS	transcriptome-wide association study
VSMC	vascular smooth muscle cell
WT	wild-type

References

1. Sillesen AS, Vøgg O, Pihl C, Raja AA, Sundberg K, Vedel C, Zingenberg H, Jørgensen FS, Vejlsstrup N, Iversen K, et al. Prevalence of Bicuspid Aortic Valve and Associated Aortopathy

- in Newborns in Copenhagen, Denmark. *Jama*. 2021;325:561–567. doi: 10.1001/jama.2020.27205 [PubMed: 33560321]
2. Movahed MR, Hepner AD, Ahmadi-Kashani M. Echocardiographic prevalence of bicuspid aortic valve in the population. *Heart, lung & circulation*. 2006;15:297–299. doi: 10.1016/j.hlc.2006.06.001
 3. Siu SC, Silversides CK. Bicuspid aortic valve disease. *Journal of the American College of Cardiology*. 2010;55:2789–2800. doi: 10.1016/j.jacc.2009.12.068 [PubMed: 20579534]
 4. Waller B, Howard J, Fess S. Pathology of aortic valve stenosis and pure aortic regurgitation. A clinical morphologic assessment--Part I. *Clinical cardiology*. 1994;17:85–92. [PubMed: 8162631]
 5. Cripe L, Andelfinger G, Martin LJ, Shooner K, Benson DW. Bicuspid aortic valve is heritable. *Journal of the American College of Cardiology*. 2004;44:138–143. doi: 10.1016/j.jacc.2004.03.050 [PubMed: 15234422]
 6. Bray JJH, Freer R, Pitcher A, Kharbanda R. Family screening for bicuspid aortic valve and aortic dilatation: a meta-analysis. *European heart journal*. 2023;44:3152–3164. doi: 10.1093/eurheartj/ehad320 [PubMed: 37288540]
 7. Bravo-Jaimes K, Prakash SK. Genetics in bicuspid aortic valve disease: Where are we? *Progress in cardiovascular diseases*. 2020;63:398–406. doi: 10.1016/j.pcad.2020.06.005 [PubMed: 32599026]
 8. Yasuhara J, Schultz K, Bigelow AM, Garg V. Congenital aortic valve stenosis: from pathophysiology to molecular genetics and the need for novel therapeutics. *Frontiers in cardiovascular medicine*. 2023;10:1142707. doi: 10.3389/fcvm.2023.1142707 [PubMed: 37187784]
 9. Delwarde C, Toquet C, Boureau AS, Le Ruz R, Le Scouarnec S, Mérot J, Kyndt F, Bernstein D, Bernstein JA, Aalberts JJJ, et al. Filamin A heart valve disease as a genetic cause of inherited bicuspid and tricuspid aortic valve disease. *Heart (British Cardiac Society)*. 2024;110:666–674. doi: 10.1136/heartjnl-2023-323491 [PubMed: 38148157]
 10. Girdauskas E, Geist L, Disha K, Kazakbaev I, Gross T, Schulz S, Ungelenk M, Kuntze T, Reichenspurner H, Kurth I. Genetic abnormalities in bicuspid aortic valve root phenotype: preliminary results. *European journal of cardio-thoracic surgery : official journal of the European Association for Cardio-thoracic Surgery*. 2017;52:156–162. doi: 10.1093/ejcts/ezx065 [PubMed: 28387797]
 11. Gillis E, Kumar AA, Luyckx I, Preuss C, Cannaeerts E, van de Beek G, Wieschendorf B, Alaerts M, Bolar N, Vandeweyer G, et al. Candidate Gene Resequencing in a Large Bicuspid Aortic Valve-Associated Thoracic Aortic Aneurysm Cohort: SMAD6 as an Important Contributor. *Frontiers in physiology*. 2017;8:400. doi: 10.3389/fphys.2017.00400 [PubMed: 28659821]
 12. Dargis N, Lamontagne M, Gaudreault N, Sbarra L, Henry C, Pibarot P, Mathieu P, Bosse Y. Identification of Gender-Specific Genetic Variants in Patients With Bicuspid Aortic Valve. *The American journal of cardiology*. 2016;117:420–426. doi: 10.1016/j.amjcard.2015.10.058 [PubMed: 26708639]
 13. Gehlen J, Stundl A, Debiec R, Fontana F, Krane M, Sharipova D, Nelson CP, Al-Kassou B, Giel AS, Sinning JM, et al. Elucidation of the genetic causes of bicuspid aortic valve disease. *Cardiovasc Res*. 2022. doi: 10.1093/cvr/cvac099
 14. Yang B, Zhou W, Jiao J, Nielsen JB, Mathis MR, Heydarpour M, Lettre G, Folkersen L, Prakash S, Schurmann C, et al. Protein-altering and regulatory genetic variants near GATA4 implicated in bicuspid aortic valve. *Nature communications*. 2017;8:15481. doi: 10.1038/ncomms15481
 15. Helgadóttir A, Thorleifsson G, Gretarsdóttir S, Stefansson OA, Tragante V, Thorolfsdóttir RB, Jonsdóttir I, Bjornsson T, Steinthorsdóttir V, Verweij N, et al. Genome-wide analysis yields new loci associating with aortic valve stenosis. *Nature communications*. 2018;9:987. doi: 10.1038/s41467-018-03252-6
 16. Willer CJ, Li Y, Abecasis GR. METAL: fast and efficient meta-analysis of genomewide association scans. *Bioinformatics (Oxford, England)*. 2010;26:2190–2191. doi: 10.1093/bioinformatics/btq340 [PubMed: 20616382]
 17. Thériault S, Li Z, Abner E, Luan J, Manikpurage HD, Houessou U, Zamani P, Briend M, Boudreau DK, Gaudreault N, et al. Integrative genomic analyses identify candidate causal genes for calcific aortic valve stenosis involving tissue-specific regulation. *Nature communications*. 2024;15:2407. doi: 10.1038/s41467-024-46639-4

18. Pirruccello JP, Chaffin MD, Chou EL, Fleming SJ, Lin H, Nekoui M, Khurshid S, Friedman SF, Bick AG, Arduini A, et al. Deep learning enables genetic analysis of the human thoracic aorta. *Nature genetics*. 2022;54:40–51. doi: 10.1038/s41588-021-00962-4 [PubMed: 34837083]
19. Bulik-Sullivan BK, Loh PR, Finucane HK, Ripke S, Yang J, Patterson N, Daly MJ, Price AL, Neale BM. LD Score regression distinguishes confounding from polygenicity in genome-wide association studies. *Nature genetics*. 2015;47:291–295. doi: 10.1038/ng.3211 [PubMed: 25642630]
20. Wang K, Li M, Hakonarson H. ANNOVAR: functional annotation of genetic variants from high-throughput sequencing data. *Nucleic acids research*. 2010;38:e164. doi: 10.1093/nar/gkq603 [PubMed: 20601685]
21. Hormozdiari F, Kostem E, Kang EY, Pasaniuc B, Eskin E. Identifying causal variants at loci with multiple signals of association. *Genetics*. 2014;198:497–508. doi: 10.1534/genetics.114.167908 [PubMed: 25104515]
22. Wang G, Sarkar A, Carbonetto P, Stephens M. A simple new approach to variable selection in regression, with application to genetic fine mapping. *Journal of the Royal Statistical Society Series B, Statistical methodology*. 2020;82:1273–1300. doi: 10.1111/rssb.12388 [PubMed: 37220626]
23. The GTEx Consortium atlas of genetic regulatory effects across human tissues. *Science (New York, NY)*. 2020;369:1318–1330. doi: 10.1126/science.aaz1776
24. Gamazon ER, Wheeler HE, Shah KP, Mozaffari SV, Aquino-Michaels K, Carroll RJ, Eyler AE, Denny JC, Nicolae DL, Cox NJ, et al. A gene-based association method for mapping traits using reference transcriptome data. *Nature genetics*. 2015;47:1091–1098. doi: 10.1038/ng.3367 [PubMed: 26258848]
25. Barbeira AN, Dickinson SP, Bonazzola R, Zheng J, Wheeler HE, Torres JM, Torstenson ES, Shah KP, Garcia T, Edwards TL, et al. Exploring the phenotypic consequences of tissue specific gene expression variation inferred from GWAS summary statistics. *Nature communications*. 2018;9:1825. doi: 10.1038/s41467-018-03621-1
26. Stegle O, Parts L, Durbin R, Winn J. A Bayesian framework to account for complex non-genetic factors in gene expression levels greatly increases power in eQTL studies. *PLoS computational biology*. 2010;6:e1000770. doi: 10.1371/journal.pcbi.1000770 [PubMed: 20463871]
27. Giambartolomei C, Vukcevic D, Schadt EE, Franke L, Hingorani AD, Wallace C, Plagnol V. Bayesian test for colocalisation between pairs of genetic association studies using summary statistics. *PLoS genetics*. 2014;10:e1004383. doi: 10.1371/journal.pgen.1004383 [PubMed: 24830394]
28. Gazal S, Weissbrod O, Hormozdiari F, Dey KK, Nasser J, Jagadeesh KA, Weiner DJ, Shi H, Fulco CP, O'Connor LJ, et al. Combining SNP-to-gene linking strategies to identify disease genes and assess disease omnigenicity. *Nature genetics*. 2022;54:827–836. doi: 10.1038/s41588-022-01087-y [PubMed: 35668300]
29. Zhou Y, Zhou B, Pache L, Chang M, Khodabakhshi AH, Tanaseichuk O, Benner C, Chanda SK. Metascape provides a biologist-oriented resource for the analysis of systems-level datasets. *Nature communications*. 2019;10:1523. doi: 10.1038/s41467-019-09234-6
30. Aleström P, D'Angelo L, Midtlyng PJ, Schorderet DF, Schulte-Merker S, Sohm F, Warner S. Zebrafish: Housing and husbandry recommendations. *Laboratory animals*. 2020;54:213–224. doi: 10.1177/0023677219869037 [PubMed: 31510859]
31. Kroll F, Powell GT, Ghosh M, Gestri G, Antinucci P, Hearn TJ, Tunbak H, Lim S, Dennis HW, Fernandez JM, et al. A simple and effective F0 knockout method for rapid screening of behaviour and other complex phenotypes. *eLife*. 2021;10. doi: 10.7554/eLife.59683
32. Privé F, Arbel J, Vilhjálmsson BJ. LDpred2: better, faster, stronger. *Bioinformatics (Oxford, England)*. 2020;36:5424–5431. doi: 10.1093/bioinformatics/btaa1029
33. Li RG, Xu YJ, Wang J, Liu XY, Yuan F, Huang RT, Xue S, Li L, Liu H, Li YJ, et al. GATA4 Loss-of-Function Mutation and the Congenitally Bicuspid Aortic Valve. *The American journal of cardiology*. 2018;121:469–474. doi: 10.1016/j.amjcard.2017.11.012 [PubMed: 29325903]
34. Faucherre A, Moha Ou Maati H, Nasr N, Pinard A, Theron A, Odelin G, Desvignes JP, Salgado D, Collod-Béroud G, Avierinos JF, et al. Piezo1 is required for outflow tract and aortic

- valve development. *Journal of molecular and cellular cardiology*. 2020;143:51–62. doi: 10.1016/j.yjmcc.2020.03.013 [PubMed: 32251670]
35. Rambeau P, Faure E, Theron A, Avierinos JF, Jopling C, Zaffran S, Faucherre A. Reduced aggrecan expression affects cardiac outflow tract development in zebrafish and is associated with bicuspid aortic valve disease in humans. *International journal of cardiology*. 2017;249:340–343. doi: 10.1016/j.ijcard.2017.09.174 [PubMed: 28986054]
 36. Paolini A, Fontana F, Pham VC, Rödel CJ, Abdelilah-Seyfried S. Mechanosensitive Notch-Dll4 and Klf2-Wnt9 signaling pathways intersect in guiding valvulogenesis in zebrafish. *Cell reports*. 2021;37:109782. doi: 10.1016/j.celrep.2021.109782 [PubMed: 34610316]
 37. Bosada FM, Devasthali V, Jones KA, Stankunas K. Wnt/ β -catenin signaling enables developmental transitions during valvulogenesis. *Development (Cambridge, England)*. 2016;143:1041–1054. doi: 10.1242/dev.130575 [PubMed: 26893350]
 38. Paolini A, Abdelilah-Seyfried S. The mechanobiology of zebrafish cardiac valve leaflet formation. *Current opinion in cell biology*. 2018;55:52–58. doi: 10.1016/j.ccb.2018.05.007 [PubMed: 30007126]
 39. Sun Z, Tseng HY, Tan S, Senger F, Kurzawa L, Dedden D, Mizuno N, Wasik AA, They M, Dunn AR, et al. Kank2 activates talin, reduces force transduction across integrins and induces central adhesion formation. *Nature cell biology*. 2016;18:941–953. doi: 10.1038/ncb3402 [PubMed: 27548916]
 40. Lemmens K, Doggen K, De Keulenaer GW. Role of neuregulin-1/ErbB signaling in cardiovascular physiology and disease: implications for therapy of heart failure. *Circulation*. 2007;116:954–960. doi: 10.1161/circulationaha.107.690487 [PubMed: 17709650]
 41. Iwamoto R, Mine N, Mizushima H, Mekada E. ErbB1 and ErbB4 generate opposing signals regulating mesenchymal cell proliferation during valvulogenesis. *Journal of cell science*. 2017;130:1321–1332. doi: 10.1242/jcs.196618 [PubMed: 28232522]
 42. Gassmann M, Casagrande F, Orioli D, Simon H, Lai C, Klein R, Lemke G. Aberrant neural and cardiac development in mice lacking the ErbB4 neuregulin receptor. *Nature*. 1995;378:390–394. doi: 10.1038/378390a0 [PubMed: 7477376]
 43. Gräf S, Haimel M, Bleda M, Hadinnapola C, Southgate L, Li W, Hodgson J, Liu B, Salmon RM, Southwood M, et al. Identification of rare sequence variation underlying heritable pulmonary arterial hypertension. *Nature communications*. 2018;9:1416. doi: 10.1038/s41467-018-03672-4
 44. Kück U, Radchenko D, Teichert I. STRIPAK, a highly conserved signaling complex, controls multiple eukaryotic cellular and developmental processes and is linked with human diseases. *Biological chemistry*. 2019;400:1005–1022. doi: 10.1515/hsz-2019-0173 [PubMed: 31042639]
 45. Lahav-Ariel L, Caspi M, Nadar-Ponniah PT, Zelikson N, Hofmann I, Hanson KK, Franke WW, Sklan EH, Avraham KB, Rosin-Arbesfeld R. Striatin is a novel modulator of cell adhesion. *FASEB journal : official publication of the Federation of American Societies for Experimental Biology*. 2019;33:4729–4740. doi: 10.1096/fj.201801882R [PubMed: 30592649]
 46. Levin MG, Tsao NL, Singhal P, Liu C, Vy HMT, Paranjpe I, Backman JD, Bellomo TR, Bone WP, Biddinger KJ, et al. Genome-wide association and multi-trait analyses characterize the common genetic architecture of heart failure. *Nature communications*. 2022;13:6914. doi: 10.1038/s41467-022-34216-6
 47. Cull JJ, Cooper STE, Alharbi HO, Chothani SP, Rackham OJL, Meijles DN, Dash PR, Kerkelä R, Ruparelia N, Sugden PH, et al. Striatin plays a major role in angiotensin II-induced cardiomyocyte and cardiac hypertrophy in mice in vivo. *Clinical science (London, England : 1979)*. 2024;138:573–597. doi: 10.1042/cs20240496 [PubMed: 38718356]
 48. Davis CA, Haberland M, Arnold MA, Sutherland LB, McDonald OG, Richardson JA, Childs G, Harris S, Owens GK, Olson EN. PRISM/PRDM6, a transcriptional repressor that promotes the proliferative gene program in smooth muscle cells. *Molecular and cellular biology*. 2006;26:2626–2636. doi: 10.1128/mcb.26.7.2626-2636.2006 [PubMed: 16537907]
 49. Li AH, Hanchard NA, Furthner D, Fernbach S, Azamian M, Nicosia A, Rosenfeld J, Muzny D, D'Alessandro LCA, Morris S, et al. Whole exome sequencing in 342 congenital cardiac left sided lesion cases reveals extensive genetic heterogeneity and complex inheritance patterns. *Genome medicine*. 2017;9:95. doi: 10.1186/s13073-017-0482-5 [PubMed: 29089047]

50. Zou M, Mangum KD, Magin JC, Cao HH, Yarboro MT, Shelton EL, Taylor JM, Reese J, Furey TS, Mack CP. Prdm6 drives ductus arteriosus closure by promoting ductus arteriosus smooth muscle cell identity and contractility. *JCI insight*. 2023;8. doi: 10.1172/jci.insight.163454
51. Klarin D, Devineni P, Sendamarai AK, Angueira AR, Graham SE, Shen YH, Levin MG, Pirruccello JP, Surakka I, Karnam PR, et al. Genome-wide association study of thoracic aortic aneurysm and dissection in the Million Veteran Program. *Nature genetics*. 2023;55:1106–1115. doi: 10.1038/s41588-023-01420-z [PubMed: 37308786]
52. Gessert S, Kühl M. The multiple phases and faces of wnt signaling during cardiac differentiation and development. *Circulation research*. 2010;107:186–199. doi: 10.1161/circresaha.110.221531 [PubMed: 20651295]
53. Hovanes K, Li TW, Waterman ML. The human LEF-1 gene contains a promoter preferentially active in lymphocytes and encodes multiple isoforms derived from alternative splicing. *Nucleic acids research*. 2000;28:1994–2003. doi: 10.1093/nar/28.9.1994 [PubMed: 10756202]
54. Alfieri CM, Cheek J, Chakraborty S, Yutzey KE. Wnt signaling in heart valve development and osteogenic gene induction. *Developmental biology*. 2010;338:127–135. doi: 10.1016/j.ydbio.2009.11.030 [PubMed: 19961844]
55. Essebiec P, Keyser M, Yordanov T, Hill B, Yu A, Noordstra I, Yap AS, Stehbens SJ, Lagendijk AK, Schimmel L, et al. c-Src-induced vascular malformations require localised matrix degradation at focal adhesions. *Journal of cell science*. 2024;137. doi: 10.1242/jcs.262101
56. Evangelou E, Warren HR, Mosen-Ansorena D, Mifsud B, Pazoki R, Gao H, Ntritsos G, Dimou N, Cabrera CP, Karaman I, et al. Genetic analysis of over 1 million people identifies 535 new loci associated with blood pressure traits. *Nature genetics*. 2018;50:1412–1425. doi: 10.1038/s41588-018-0205-x [PubMed: 30224653]
57. Jiang X, Hysi PG, Khawaja AP, Mahroo OA, Xu Z, Hammond CJ, Foster PJ, Welikala RA, Barman SA, Whincup PH, et al. GWAS on retinal vasculometry phenotypes. *PLoS genetics*. 2023;19:e1010583. doi: 10.1371/journal.pgen.1010583 [PubMed: 36757925]
58. Bainbridge MN, Davis EE, Choi WY, Dickson A, Martinez HR, Wang M, Dinh H, Muzny DM, Pignatelli R, Katsanis N, et al. Loss of Function Mutations in NNT Are Associated With Left Ventricular Noncompaction. *Circulation Cardiovascular genetics*. 2015;8:544–552. doi: 10.1161/circgenetics.115.001026 [PubMed: 26025024]
59. Karamanavi E, McVey DG, van der Laan SW, Stanczyk PJ, Morris GE, Wang Y, Yang W, Chan K, Poston RN, Luo J, et al. The FES Gene at the 15q26 Coronary-Artery-Disease Locus Inhibits Atherosclerosis. *Circulation research*. 2022;131:1004–1017. doi: 10.1161/circresaha.122.321146 [PubMed: 36321446]
60. Krzesi ska A, Nowak M, Mickiewicz A, Chyla-Danił G, wikli ska A, Koper-Lenkiewicz OM, Kami ska J, Matowicka-Karna J, Gruchała M, Jankowski M, et al. Lipoprotein(a) As a Potential Predictive Factor for Earlier Aortic Valve Replacement in Patients with Bicuspid Aortic Valve. *Biomedicines*. 2023;11. doi: 10.3390/biomedicines11071823
61. Garg V, Muth AN, Ransom JF, Schluterman MK, Barnes R, King IN, Grossfeld PD, Srivastava D. Mutations in NOTCH1 cause aortic valve disease. *Nature*. 2005;437:270–274. doi: 10.1038/nature03940 [PubMed: 16025100]
62. Ducharme V, Guaque-Olarte S, Gaudreault N, Pibarot P, Mathieu P, Bosse Y. NOTCH1 genetic variants in patients with tricuspid calcific aortic valve stenosis. *The Journal of heart valve disease*. 2013;22:142–149. [PubMed: 23798201]
63. Thériault S, Dina C, Messika-Zeitoun D, Le Scouarnec S, Capoulade R, Gaudreault N, Rigade S, Li Z, Simonet F, Lamontagne M, et al. Genetic Association Analyses Highlight IL6, ALPL, and NAV1 As 3 New Susceptibility Genes Underlying Calcific Aortic Valve Stenosis. *Circulation Genomic and precision medicine*. 2019;12:e002617. doi: 10.1161/circgen.119.002617 [PubMed: 32141789]
64. Boureau AS, Karakachoff M, Le Scouarnec S, Capoulade R, Cuffe C, de Decker L, Senage T, Verhoye JP, Baufreton C, Roussel JC, et al. Heritability of aortic valve stenosis and bicuspid enrichment in families with aortic valve stenosis. *International journal of cardiology*. 2022;359:91–98. doi: 10.1016/j.ijcard.2022.04.022 [PubMed: 35427703]
65. Carlisle SG, Albasha H, Michelena HI, Sabate-Rotes A, Bianco L, De Backer J, Mosquera LM, Yetman AT, Bissell MM, Andreassi MG, et al. Rare genomic copy number variants

- implicate new candidate genes for bicuspid aortic valve. *PLoS one*. 2024;19:e0304514. doi: 10.1371/journal.pone.0304514 [PubMed: 39240962]
66. Khera AV, Chaffin M, Aragam KG, Haas ME, Roselli C, Choi SH, Natarajan P, Lander ES, Lubitz SA, Ellinor PT, et al. Genome-wide polygenic scores for common diseases identify individuals with risk equivalent to monogenic mutations. *Nature genetics*. 2018;50:1219–1224. doi: 10.1038/s41588-018-0183-z [PubMed: 30104762]
 67. Small AM, Melloni GEM, Kamanu FK, Bergmark BA, Bonaca MP, O'Donoghue ML, Giugliano RP, Scirica BM, Bhatt D, Antman EM, et al. Novel Polygenic Risk Score and Established Clinical Risk Factors for Risk Estimation of Aortic Stenosis. *JAMA cardiology*. 2024;9:357–366. doi: 10.1001/jamacardio.2024.0011 [PubMed: 38416462]
 68. Chandra S, Lang RM, Nicolarsen J, Gayat E, Spencer KT, Mor-Avi V, Hofmann Bowman MA. Bicuspid aortic valve: inter-racial difference in frequency and aortic dimensions. *JACC Cardiovascular imaging*. 2012;5:981–989. doi: 10.1016/j.jcmg.2012.07.008 [PubMed: 23058064]
 69. Balkau B, Lange C, Fezeu L, Tichet J, de Lauzon-Guillain B, Czernichow S, Fumeron F, Froguel P, Vaxillaire M, Cauchi S, et al. Predicting diabetes: clinical, biological, and genetic approaches: data from the Epidemiological Study on the Insulin Resistance Syndrome (DESIR). *Diabetes care*. 2008;31:2056–2061. doi: 10.2337/dc08-0368 [PubMed: 18689695]
 70. Bezzina CR, Barc J, Mizusawa Y, Remme CA, Gourraud JB, Simonet F, Verkerk AO, Schwartz PJ, Crotti L, Dagradi F, et al. Common variants at SCN5A-SCN10A and HEY2 are associated with Brugada syndrome, a rare disease with high risk of sudden cardiac death. *Nature genetics*. 2013;45:1044–1049. doi: 10.1038/ng.2712 [PubMed: 23872634]
 71. Alves I, Gienza J, Blum MGB, Bernhardsson C, Chatel S, Karakachoff M, Saint Pierre A, Herzig AF, Olaso R, Monteil M, et al. Human genetic structure in Northwest France provides new insights into West European historical demography. *Nature communications*. 2024;15:6710. doi: 10.1038/s41467-024-51087-1
 72. Herzig AF, Velo-Suárez L, Dina C, Redon R, Deleuze JF, Génin E. How local reference panels improve imputation in French populations. *Scientific reports*. 2024;14:370. doi: 10.1038/s41598-023-49931-3 [PubMed: 38172507]
 73. Awadalla P, Boileau C, Payette Y, Idaghmour Y, Goulet JP, Knoppers B, Hamet P, Laberge C. Cohort profile of the CARTaGENE study: Quebec's population-based biobank for public health and personalized genomics. *International journal of epidemiology*. 2013;42:1285–1299. doi: 10.1093/ije/dys160 [PubMed: 23071140]
 74. Roychowdhury T, Lu H, Hornsby WE, Crone B, Wang GT, Guo DC, Sendamarai AK, Devineni P, Lin M, Zhou W, et al. Regulatory variants in TCF7L2 are associated with thoracic aortic aneurysm. *American journal of human genetics*. 2021;108:1578–1589. doi: 10.1016/j.ajhg.2021.06.016 [PubMed: 34265237]
 75. Schermund A, Möhlenkamp S, Stang A, Grönemeyer D, Seibel R, Hirche H, Mann K, Siffert W, Lauterbach K, Siegrist J, et al. Assessment of clinically silent atherosclerotic disease and established and novel risk factors for predicting myocardial infarction and cardiac death in healthy middle-aged subjects: rationale and design of the Heinz Nixdorf RECALL Study. *Risk Factors, Evaluation of Coronary Calcium and Lifestyle*. *American heart journal*. 2002;144:212–218. doi: 10.1067/mhj.2002.123579 [PubMed: 12177636]
 76. Kurki MI, Karjalainen J, Palta P, Sipilä TP, Kristiansson K, Donner KM, Reeve MP, Laivuori H, Aavikko M, Kaunisto MA, et al. FinnGen provides genetic insights from a well-phenotyped isolated population. *Nature*. 2023;613:508–518. doi: 10.1038/s41586-022-05473-8 [PubMed: 36653562]
 77. Genomic data in the All of Us Research Program. *Nature*. 2024;627:340–346. doi: 10.1038/s41586-023-06957-x [PubMed: 38374255]
 78. Bycroft C, Freeman C, Petkova D, Band G, Elliott LT, Sharp K, Motyer A, Vukcevic D, Delaneau O, O'Connell J, et al. The UK Biobank resource with deep phenotyping and genomic data. *Nature*. 2018;562:203–209. doi: 10.1038/s41586-018-0579-z [PubMed: 30305743]
 79. Chang CC, Chow CC, Tellier LC, Vattikuti S, Purcell SM, Lee JJ. Second-generation PLINK: rising to the challenge of larger and richer datasets. *GigaScience*. 2015;4:7. doi: 10.1186/s13742-015-0047-8 [PubMed: 25722852]

80. Bowden J, Del Greco MF, Minelli C, Zhao Q, Lawlor DA, Sheehan NA, Thompson J, Davey Smith G. Improving the accuracy of two-sample summary-data Mendelian randomization: moving beyond the NOME assumption. *International journal of epidemiology*. 2019;48:728–742. doi: 10.1093/ije/dyy258 [PubMed: 30561657]
81. Bowden J, Davey Smith G, Burgess S. Mendelian randomization with invalid instruments: effect estimation and bias detection through Egger regression. *International journal of epidemiology*. 2015;44:512–525. doi: 10.1093/ije/dyv080 [PubMed: 26050253]
82. Bowden J, Davey Smith G, Haycock PC, Burgess S. Consistent Estimation in Mendelian Randomization with Some Invalid Instruments Using a Weighted Median Estimator. *Genetic epidemiology*. 2016;40:304–314. doi: 10.1002/gepi.21965 [PubMed: 27061298]
83. Trapnell C, Pachter L, Salzberg SL. TopHat: discovering splice junctions with RNA-Seq. *Bioinformatics (Oxford, England)*. 2009;25:1105–1111. doi: 10.1093/bioinformatics/btp120 [PubMed: 19289445]
84. Langmead B, Trapnell C, Pop M, Salzberg SL. Ultrafast and memory-efficient alignment of short DNA sequences to the human genome. *Genome biology*. 2009;10:R25. doi: 10.1186/gb-2009-10-3-r25 [PubMed: 19261174]
85. Wagner GP, Kin K, Lynch VJ. Measurement of mRNA abundance using RNA-seq data: RPKM measure is inconsistent among samples. *Theory in biosciences = Theorie in den Biowissenschaften*. 2012;131:281–285. doi: 10.1007/s12064-012-0162-3 [PubMed: 22872506]
86. Odelin G, Faucherre A, Marchese D, Pinard A, Jaouadi H, Le Scouarnec S, Chiarelli R, Achouri Y, Faure E, Herbane M, et al. Variations in the poly-histidine repeat motif of HOXA1 contribute to bicuspid aortic valve in mouse and zebrafish. *Nature communications*. 2023;14:1543. doi: 10.1038/s41467-023-37110-x
87. Paolini A, Sharipova D, Lange T, Abdelilah-Seyfried S. Wnt9 directs zebrafish heart tube assembly via a combination of canonical and non-canonical pathway signaling. *Development (Cambridge, England)*. 2023;150. doi: 10.1242/dev.201707
88. Livak KJ, Schmittgen TD. Analysis of relative gene expression data using real-time quantitative PCR and the 2⁻(Delta Delta C(T)) Method. *Methods (San Diego, Calif)*. 2001;25:402–408. doi: 10.1006/meth.2001.1262 [PubMed: 11846609]
89. Lepiller S, Laurens V, Bouchot A, Herbomel P, Solary E, Chluba J. Imaging of nitric oxide in a living vertebrate using a diamino-fluorescein probe. *Free radical biology & medicine*. 2007;43:619–627. doi: 10.1016/j.freeradbiomed.2007.05.025 [PubMed: 17640572]
90. Renz M, Otten C, Faurobert E, Rudolph F, Zhu Y, Boulday G, Duchene J, Mickoleit M, Dietrich AC, Ramspacher C, et al. Regulation of β 1 integrin-Klf2-mediated angiogenesis by CCM proteins. *Developmental cell*. 2015;32:181–190. doi: 10.1016/j.devcel.2014.12.016 [PubMed: 25625207]
91. Beis D, Bartman T, Jin SW, Scott IC, D'Amico LA, Ober EA, Verkade H, Frantsve J, Field HA, Wehman A, et al. Genetic and cellular analyses of zebrafish atrioventricular cushion and valve development. *Development (Cambridge, England)*. 2005;132:4193–4204. doi: 10.1242/dev.01970 [PubMed: 16107477]
92. Robin X, Turck N, Hainard A, Tiberti N, Lisacek F, Sanchez JC, Müller M. pROC: an open-source package for R and S+ to analyze and compare ROC curves. *BMC bioinformatics*. 2011;12:77. doi: 10.1186/1471-2105-12-77 [PubMed: 21414208]

Clinical Perspective

What Is New?

- Through an international genome-wide association study meta-analysis, we identified 32 novel genetic regions associated with bicuspid aortic valve and prioritized *WNT4*, *LEF1*, *STRN* and *KANK2* from transcriptomic analyses and a zebrafish model.
- We developed the first polygenic risk score for bicuspid aortic valve, which was also associated with related complications.

What Are the Clinical Implications?

- The identification of genes and pathways could lead to the development of prognostic markers and personalized management in individuals with a bicuspid aortic valve.
- A polygenic risk score could help to identify individuals at risk of this congenital heart defect and its complications.

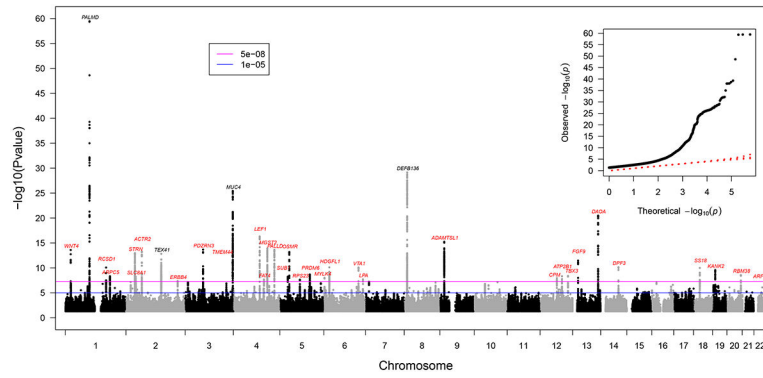


Figure 1: Manhattan plot of the genome-wide association studies meta-analysis for BAV. The nearest gene at each genome-wide significant locus is indicated, in black for known loci and in red for novel loci. The association of each variant with BAV was obtained from an inverse-variance weighted fixed-effect meta-analysis combining the effect per allele in the cohorts with available data. A p-value below 5.0×10^{-8} was considered significant (genome-wide threshold). The genomic inflation factor was 1.066 and the LD score regression intercept was 1.029. The quantile-quantile plot (inset) illustrates the distribution of p-values for all variants tested.

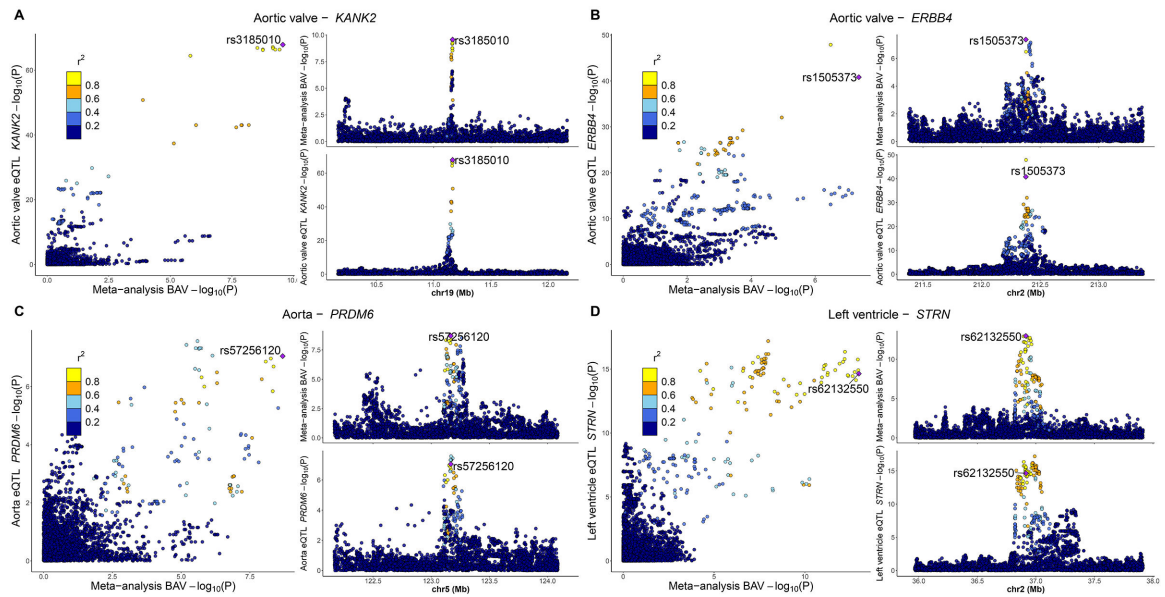


Figure 2: Transcriptomic analyses identify novel candidate causal genes at genome-wide significant loci.

LocusCompare plots showing the p-value distribution for the GWAS meta-analysis and tissue eQTLs at 4 loci. **A**, *KANK2* locus, expression in aortic valve. **B**, *ERBB4* locus, expression in aortic valve. **C**, *PRDM6* locus, expression in aorta. **D**, *STRN* locus, expression in heart left ventricle. P for bicuspid aortic valve was obtained from the inverse-variance weighted fixed-effect GWAS meta-analysis. P for eQTL was obtained from the nominal association between genotype and normalized gene expression.

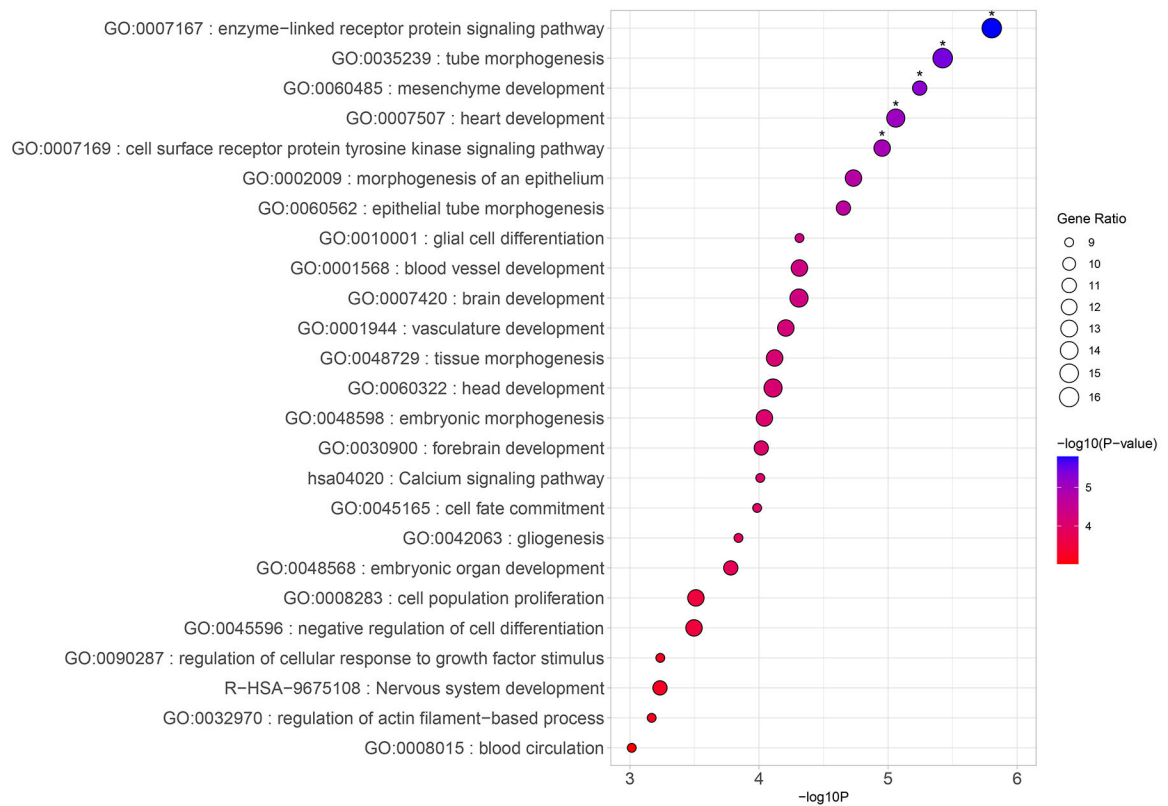


Figure 3: Pathway enrichment for candidate genes.

Bubble plot showing the enriched terms for the 55 candidate genes selected based on variant annotation and transcriptomic analyses. The terms were selected from Gene Ontology biological processes, KEGG pathways, Reactome gene sets, canonical pathways, and WikiPathways. The analysis was performed using Metascape. The statistical significance of the association for each term was obtained from a hypergeometric test and is illustrated by the color (p-value). The gene ratio is illustrated by the size of the bubble. *: terms enriched at false discovery rate < 5%.

Gene	Number of features	Nearest gene	Missense	cS2G	eQTL	TWAS	COLOC	MR	Foetal valve expression	Monogenic
<i>PRDM6</i>	8	Black	Grey	Black	Magenta	Magenta	Black	Magenta	Black	Black
<i>ATP13A3</i>	7	Grey	Grey	Black	Magenta	Magenta	Black	Magenta	Black	Black
<i>ERBB4</i>	7	Black	Grey	Black	Blue	Blue	Black	Blue	Black	Grey
<i>STRN</i>	7	Black	Grey	Black	Blue	Blue	Black	Blue	Black	Grey
<i>ARPC5</i>	6	Black	Grey	Grey	Blue	Blue	Black	Blue	Black	Grey
<i>KANK2</i>	6	Black	Grey	Black	Blue	Blue	Black	Blue	Grey	Grey
<i>LEF1</i>	6	Black	Grey	Black	Blue	Blue	Black	Grey	Black	Grey
<i>MUC4</i>	6	Black	Black	Black	Magenta	Magenta	Grey	Grey	Black	Grey
<i>RBM38</i>	6	Black	Grey	Black	Blue	Blue	Black	Grey	Black	Grey
<i>SLC8A1</i>	6	Black	Grey	Black	Blue	Blue	Black	Grey	Black	Grey
<i>ACTR2</i>	5	Black	Grey	Black	Magenta	Magenta	Black	Grey	Grey	Grey
<i>MGST2</i>	5	Black	Grey	Black	Magenta	Magenta	Black	Grey	Grey	Grey
<i>PALMD</i>	5	Black	Grey	Black	Blue	Blue	Black	Grey	Grey	Grey

Figure 4: Genes with multiple features suggesting their implication in BAV.

Summary matrix showing the candidate genes with five or more features. Nearest gene: gene closest to a lead SNP in the GWAS meta-analysis; Missense: lead GWAS SNP is in linkage disequilibrium ($r^2 > 0.8$) with a missense variant for the gene; cS2G: gene prioritized by the combined SNP-to-gene strategy with a high probability (> 0.6); eQTL: significant expression quantitative trait locus in human aortic valve, aorta, heart left ventricle or right atrial appendage at false-discovery rate $< 5\%$; TWAS: significant in transcriptome-wide association study at false discovery rate $< 5\%$; COLOC: colocalization $PP4 > 0.75$; MR: significant in inverse-variance weighting Mendelian randomization analyses at false-discovery rate $< 5\%$ and no evidence of pleiotropy (Egger intercept $P > 0.01$); Foetal valve expression: gene has higher expression in foetal compared to adult aortic valve at false discovery rate $< 5\%$ using a two-tailed, unpaired t-test; Monogenic: gene associated with a monogenic condition involving the heart or great vessels in the Online Mendelian Inheritance in Man (OMIM); Magenta squares indicate a significant positive association between gene expression and disease risk; Blue squares indicate a significant negative association between

gene expression and disease risk; Black squares implicate genes from approaches without direction of effect inference.

Author Manuscript

Author Manuscript

Author Manuscript

Author Manuscript

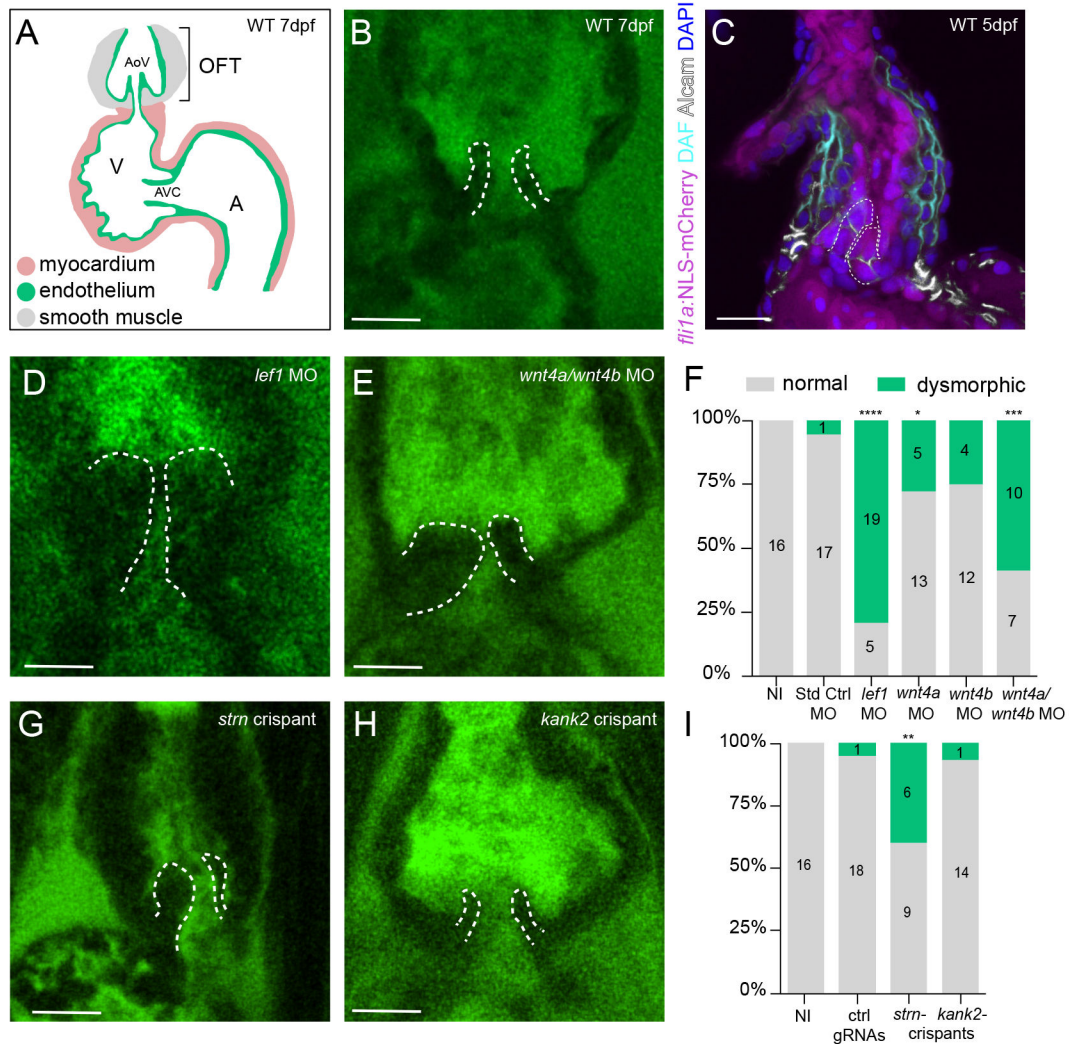


Figure 5. Outflow tract valve defects in zebrafish models of GWAS candidate genes.

A. Scheme of the zebrafish heart at 7 days post-fertilization (dpf). The two-chambered heart has one outflow tract region (OFT) where a two-leafed aortic valve (AoV) has formed. The OFT endothelium is surrounded by a thickened layer of smooth muscle cells. The atrioventricular canal (AVC) is a narrowing of the heart tube located between the ventricle (V) and the atrium (A). Here, an AVC valve has formed. **B.** Representative two-photon image of the wild-type OFT at 7 dpf labeled with BODIPY ceramide. Valve leaflets are outlined with a dashed white line. **C.** Representative confocal microscopic image of wild-type OFT whole-mount immunohistochemistry staining at 5 dpf labeled with mCherry (endocardium), DAF (smooth muscle cells), Alcain (myocardium and endothelial valve leaflets) and DAPI (nuclei). **D, E, G, H.** Representative two-photon images of OFT valves in 7 dpf *lef1* morphants (D), *wnt4a/wnt4b* double morphants (E), *strn* crispants (G), and *kank2* crispants (H), labeled with BODIPY ceramide. Valve leaflets are outlined with a dashed white line. **F, I.** Quantifications of OFT valve defects observed in 7 dpf larvae after knockdown of *lef1* (n=24), *wnt4a* (n=18), *wnt4b* (n=16) or *wnt4a+wnt4b* (n=17) compared to non-injected (NI) controls (n=16) and standard control morpholinos (n=18) (F) and in

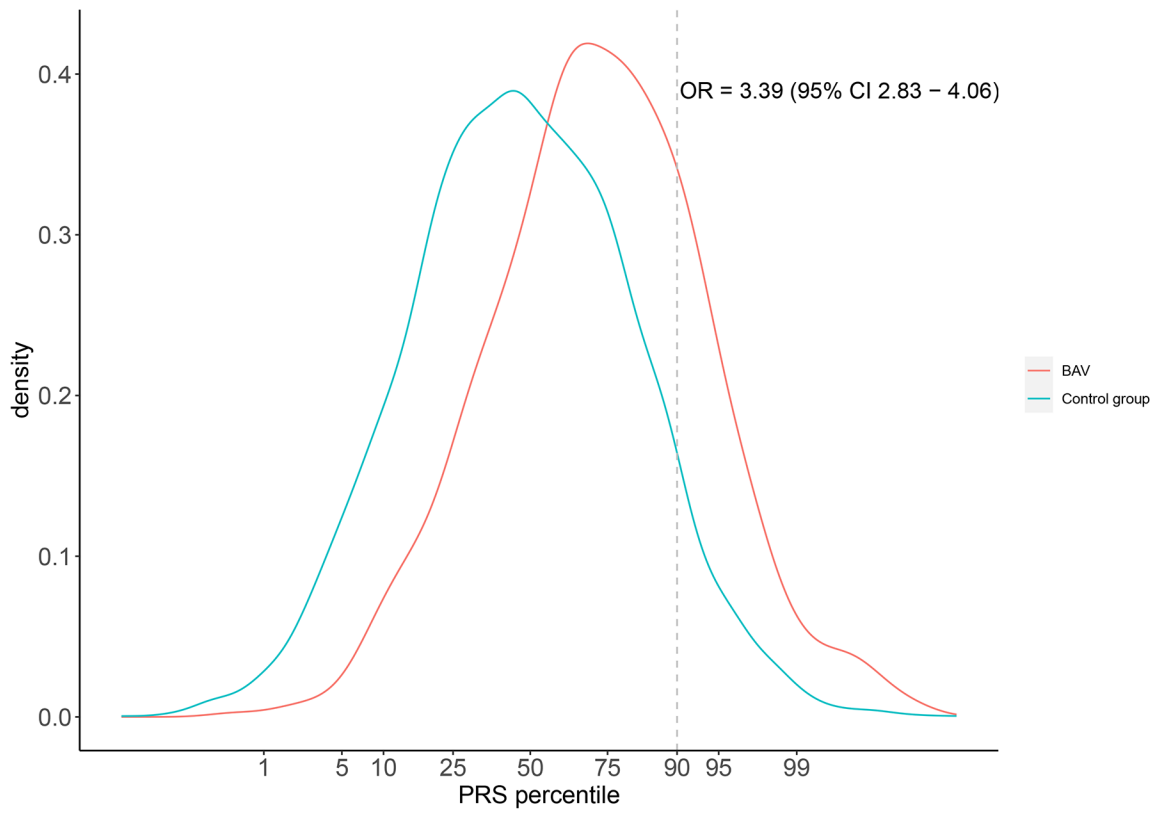
strn (n=15) and *kank2* (n=15) crispants compared to non-injected (NI) controls (n=16) and control gRNAs (n=19) (I). * $P < 0.05$, ** $P < 0.01$, *** $P < 0.001$, **** $P < 0.0001$; two-sided Fisher's exact test. Scale bars: 15 μm .

Author Manuscript

Author Manuscript

Author Manuscript

Author Manuscript

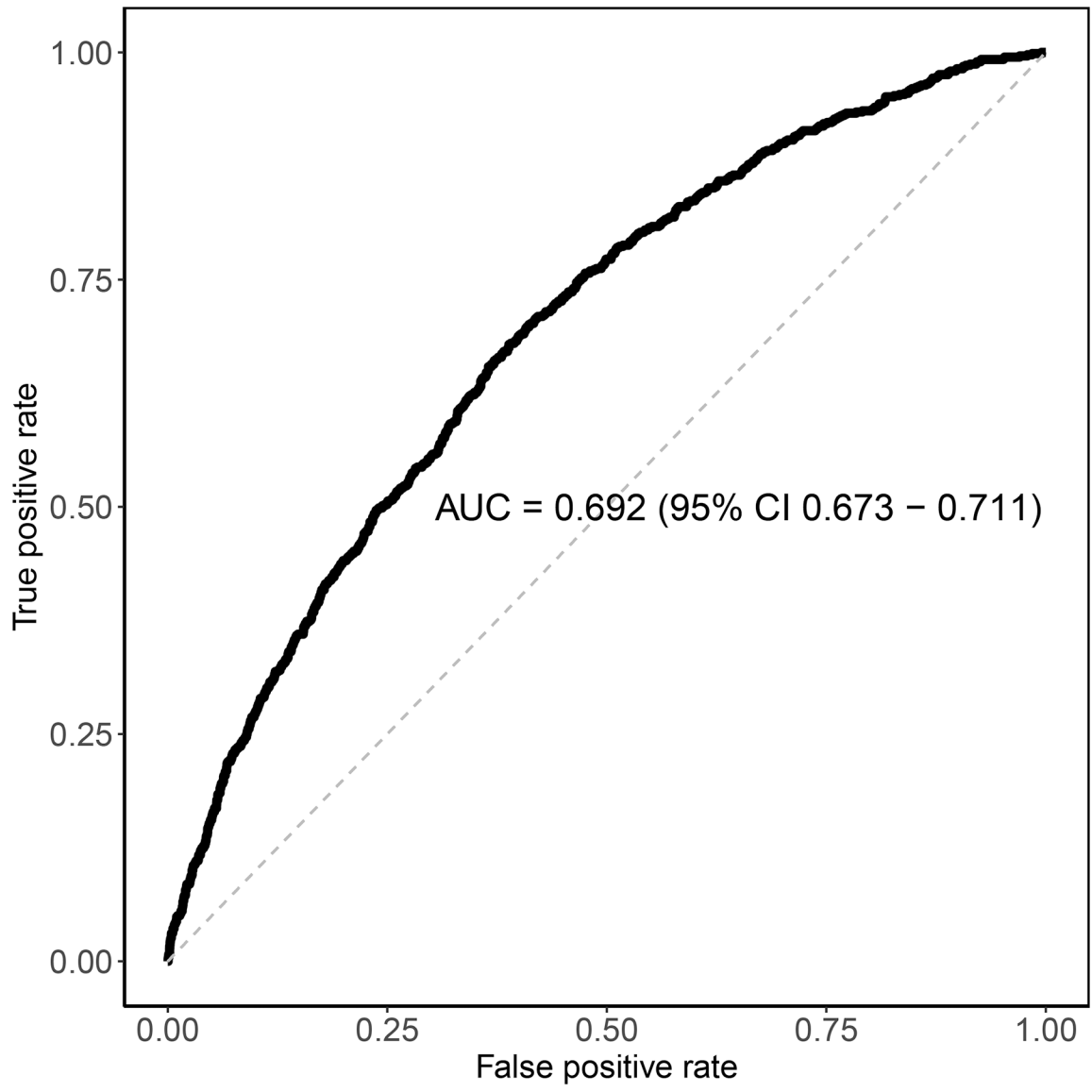


Author Manuscript

Author Manuscript

Author Manuscript

Author Manuscript



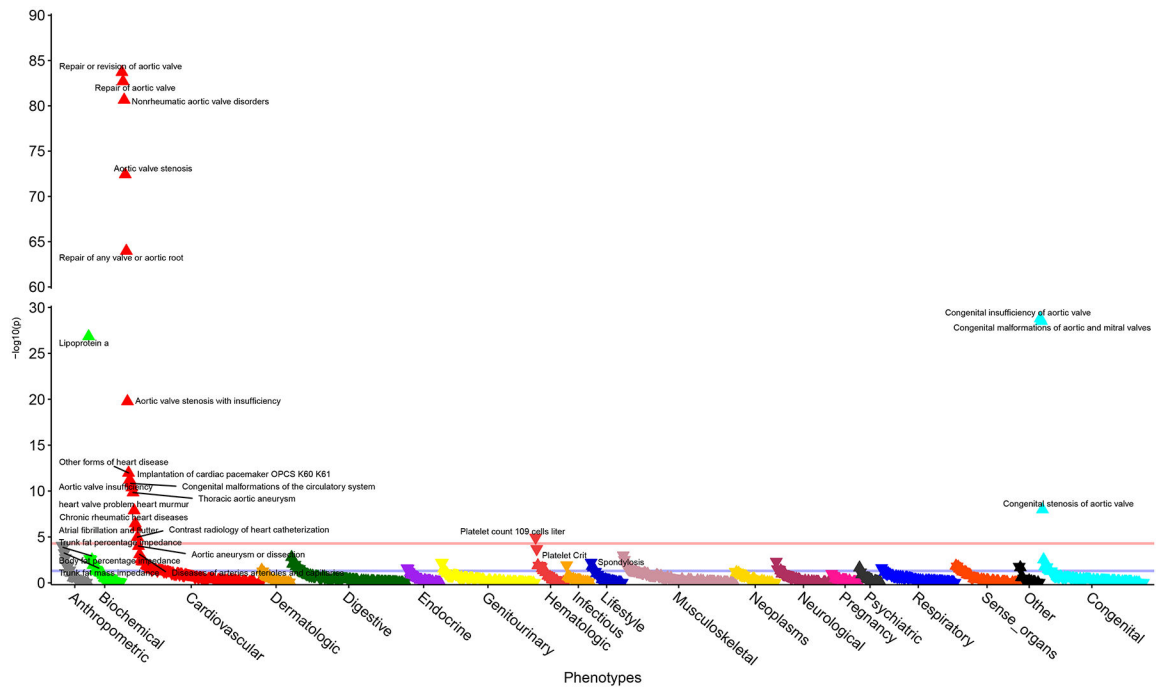


Figure 6: A polygenic risk score is associated with BAV and other cardiovascular phenotypes.

A, Distribution of the normalized polygenic risk score (PRS) in cases of BAV ($n=778$) and controls ($n=5,446$) from QUEBEC-BAV / CARTaGENE. The dashed line represents the 90th percentile of the distribution in controls. **B**, Receiver operating characteristic curve showing the capacity of the PRS to identify BAV in QUEBEC-BAV / CARTaGENE. The dashed line represents an area under the curve (AUC) of 0.5 (no ability to identify BAV). **C**, Association between the PRS derived from the complete meta-analysis and 976 phenotypes in UK Biobank using logistic or linear regression. The triangles represent the direction of effect (up indicates a positive association and down indicates a negative association). Phenotypes significantly associated with the PRS at false-discovery rate $<5\%$ are labeled. The red line corresponds to a p -value of 5.1×10^{-5} (Bonferroni threshold). The blue line corresponds to a p -value of 0.05.

Table 1. Genome-wide significant loci for BAV

Locus	rsID	Chr	Pos	RA/NRA	RAF	OR (95% CI)	P	I ² (%)	P _{Het}	Gene	Novel
1	rs116386356	1	22262631	C/T	0.069	1.29 (1.21 - 1.37)	2.57E-14	32.9	0.155	WNT4	Yes
2	rs11166276	1	99579683	T/C	0.495	1.35 (1.30 - 1.39)	3.52E-60	6.8	0.378	PALMD	No
3	rs926521	1	167623295	T/C	0.451	1.12 (1.08 - 1.16)	8.39E-11	0	0.439	RCSDI	Yes
4	rs2761557	1	183610464	C/T	0.642	1.11 (1.07 - 1.15)	4.64E-09	0	0.810	ARPC5	Yes
5	rs62132550	2	36913942	C/T	0.560	1.14 (1.10 - 1.18)	1.08E-13	29.2	0.185	STRN	Yes
6	rs12613022	2	40346783	G/A	0.629	1.11 (1.07 - 1.15)	5.51E-09	0	0.751	SLC8A1	Yes
7	rs6715876	2	65259794	C/T	0.367	1.14 (1.10 - 1.18)	5.43E-14	0	0.515	ACTR2	Yes
8	rs7593336	2	145078862	G/A	0.427	1.14 (1.10 - 1.18)	1.51E-13	18.2	0.280	ZEB2*	No
9	rs1505373	2	212377960	C/T	0.585	1.10 (1.06 - 1.14)	4.33E-08	0	0.555	ERBB4	Yes
10	rs11128363	3	73695511	C/A	0.739	1.18 (1.13 - 1.23)	2.12E-14	0	0.474	PDZRN3	Yes
11	rs1706003	3	194579238	G/T	0.569	1.17 (1.12 - 1.22)	3.79E-13	0	0.788	TMEM44	Yes
12	rs2246771	3	195760866	A/G	0.340	1.22 (1.18 - 1.27)	3.75E-26	0	0.903	MUC4	No
13	rs12502542	4	108216398	G/A	0.582	1.16 (1.12 - 1.20)	4.82E-17	0	0.865	LEFI	Yes
14	rs10034133	4	125788461	C/T	0.455	1.10 (1.07 - 1.14)	2.07E-08	0	0.444	FAT4	Yes
15	rs114728151	4	139740573	C/T	0.927	1.30 (1.21 - 1.39)	1.23E-14	35.9	0.131	MGST2, MAML3	Yes
16	rs7676725	4	168739540	A/G	0.494	1.14 (1.10 - 1.18)	2.26E-14	25	0.221	PALLD	Yes
17	rs67041063	5	32617685	A/G	0.708	1.12 (1.08 - 1.16)	5.65E-09	38.7	0.110	SUB1	Yes
18	rs4869594	5	38731246	A/C	0.390	1.14 (1.10 - 1.18)	6.35E-14	1	0.425	OSMR	Yes
19	rs58547370	5	82373029	A/G	0.108	1.17 (1.11 - 1.23)	2.27E-08	0	0.948	RPS23	Yes
20	rs57256120	5	123168317	G/A	0.289	1.12 (1.08 - 1.16)	2.03E-09	0	0.906	PRDM6	Yes
21	rs9378715	6	2573580	G/A	0.271	1.12 (1.08 - 1.16)	9.76E-09	0	0.782	MYLK4	Yes
22	rs11751669	6	22570808	A/G	0.730	1.13 (1.09 - 1.18)	7.68E-11	21.8	0.249	HDGFLI	Yes
23	rs62430519	6	142273695	C/T	0.305	1.15 (1.10 - 1.20)	8.40E-11	0	0.827	VTAI	Yes
24	rs118039278	6	160564494	A/G	0.068	1.21 (1.13 - 1.29)	1.94E-08	41.9	0.088	LPA	Yes
25	rs118065347	8	11942355	G/A	0.044	1.59 (1.47 - 1.73)	7.19E-30	41.4	0.091	DEFB136	No
26	rs1755290	9	17939172	T/C	0.597	1.16 (1.12 - 1.20)	5.68E-16	30.4	0.175	ADAMTSL1	Yes
27	rs10878881	12	68960853	C/T	0.649	1.11 (1.07 - 1.15)	1.12E-08	0	0.744	CPM	Yes
28	rs7307097	12	89946230	G/A	0.746	1.15 (1.10 - 1.20)	4.68E-09	37.6	0.129	ATP2B1	Yes

Locus	rsID	Chr	Pos	RA/NRA	RAF	OR (95% CI)	P	I ² (%)	P _{Het}	Gene	Novel
29	rs567223	12	114672766	G/T	0.483	1.12 (1.08 - 1.16)	4.03E-09	30.6	0.173	TBX3	Yes
30	rs9506819	13	22286130	T/G	0.421	1.13 (1.09 - 1.16)	3.44E-12	14.6	0.312	FGF9	Yes
31	rs735722	13	104571923	T/C	0.287	1.19 (1.15 - 1.24)	3.24E-21	0	0.958	DAOA	Yes
32	rs759283	14	72889599	A/C	0.340	1.12 (1.09 - 1.16)	7.26E-11	21.6	0.251	DPP3	Yes
33	rs9960148	18	25837395	G/T	0.625	1.12 (1.08 - 1.16)	1.01E-10	0	0.854	SS/8	Yes
34	rs3185010	19	11165166	G/A	0.684	1.13 (1.09 - 1.17)	2.70E-10	0	0.972	KANK2	Yes
35	rs574693724	20	57443143	C/CG	0.421	1.14 (1.09 - 1.20)	2.76E-09	0	0.431	RBM38	Yes
36	rs117651913	22	42854060	T/A	0.017	1.60 (1.36 - 1.89)	3.05E-08	0	0.892	ARFGAP3	Yes

Pos: position according to GRCh38; RA: risk allele; NRA: non-risk allele; RAF: risk allele frequency; I²: heterogeneity statistic; P_{Het}: heterogeneity P-value; Gene: Nearest protein-coding gene
 Genes in bold were prioritized by the cS2G analysis

* Located in lncRNA *TEX4I*